This is the accepted manuscript made available via CHORUS. The article has been published as:

Scattering phase-shift formulas for mesons and baryons in elongated boxes

Frank X. Lee and Andrei Alexandru

Phys. Rev. D **96**, 054508 — Published 11 September 2017

DOI: 10.1103/PhysRevD.96.054508

Scattering phaseshift formulas for mesons and baryons in elongated boxes

Frank X. Lee[1] and Andrei Alexandru[1, 2, *]

[1]Physics Department, The George Washington University, Washington, DC 20052, USA[†]

[2]Albert Einstein Center for Fundamental Physics, Institute for Theoretical Physics, University of Bern, Sidlerstrasse 5, CH-3012 Bern, Switzerland

We derive Lüscher phaseshift formulas for two-particle states in boxes elongated in one of the dimensions. Such boxes offer a cost-effective way of varying the relative momentum of the particles. Boosted states in the elongated direction, which allow wider access to energies, are also considered. The formulas for the various scenarios (moving and zero-momentum states in cubic and elongated boxes) are compared and relations between them are clarified. The results are applicable to a wide set of meson-meson and meson-baryon elastic scattering processes, with the two-particle system having equal or unequal masses.

PACS numbers: 12.38.Gc, 02.20.-a, 03.65.Nk, 11.80.Et

I. INTRODUCTION

Hadron-hadron scattering is an indispensable tool in understanding the nature of the strong nuclear force, both experimentally and theoretically. The theoretical groundwork was laid out by Lüscher [1] who showed how to relate elastic scattering phaseshifts with the energies of the two-body states in a finite box. Various extensions to the method have since been made to enhance its applications, including moving frames [2], moving frame involving unequal masses and baryons [3–5], asymmetric boxes [6], and more recently inelastic scattering [7, 8]. The use of asymmetric boxes has proven to be efficient in recent studies of the ρ meson resonance in $\pi\pi$ scattering [9, 10]. Instead of varying the size of the entire box, only one side is elongated, requiring much less computing resources. Our main goal in this work is to derive the phaseshift formulas needed to study meson-baryon elastic scattering in elongated boxes, with an eye towards a lattice QCD simulation of the Δ resonance in πN scattering.

II. PHASESHIFT FORMALISM

In infinite volume, standard quantum mechanics defines elastic scattering phaseshift as the change in phase in the scattered wave relative to the incident wave in the asymptotic region where the interaction can be neglected. In the partial-wave expansion, the wavefunction is $\psi(\boldsymbol{r}) = e^{ikz} + f(\theta)\frac{e^{ikr}}{r}$ where $f(\theta) = \sum_{l=0}^{\infty}(2l+1)f_l P_l(\cos\theta)$ is the scattering amplitude, and phaseshift δ_l enters via $f_l = \frac{e^{2i\delta_l}-1}{2ik}$. The phaseshift is a real-valued function of the interaction energy and carries information about the nature of the interaction, such as whether the force is attractive ($\delta < 0$) or repulsive ($\delta > 0$), whether a resonance is formed in the scattering, etc. Scattering length can also be extracted in its effective range expansion. The phaseshift can be determined in the region where the interaction is vanishing, so the solution to the Schrödinger equation (which has the form of a Helmholtz equation)

$$(\nabla^2 + k^2)\psi(\boldsymbol{r}) = 0\,, \tag{1}$$

can be expressed in terms of ordinary spherical bessel functions $\psi \propto [\alpha_l j_l(kr) + \beta_l n_l(kr)]$ where the coefficients can be found by matching up with the wavefunction in the interior. The phaseshift can be computed from the coefficients by

$$e^{2i\delta_l(k)} = \frac{\alpha_l(k) + i\beta_l(k)}{\alpha_l(k) - i\beta_l(k)}\,. \tag{2}$$

On the lattice, a similar procedure can be followed to study scattering phaseshifts as shown by Lüscher, except that the system is now confined in a box of size L (we assume the size is big enough so that the interaction range $R < L/2$). The wavefunction must satisfy periodic boundary conditions

$$\psi(\boldsymbol{r} + \boldsymbol{n}L) = \psi(\boldsymbol{r}) \tag{3}$$

so the solutions to the Helmholtz equation are zeta functions instead of Bessel functions. Basically, one ends up with a new relation that connects the phaseshifts with the energies of two-body states in the box, in the form of a matrix equation [1]

$$\det\left[e^{2i\delta(k,L)} - \frac{\mathcal{M}(k,L) + i}{\mathcal{M}(k,L) - i}\right] = 0\,, \tag{4}$$

for positive relative momentum k. The $\mathcal{M}(k,L)$ is a well-defined matrix in terms of zeta functions, and it is purely a mathematical function of the relative momentum and box geometry.

The Lüscher method provides a general strategy to understand hadron resonances via the phaseshift from the first principles of QCD. The basic idea is to take advantage of the dependence of the phaseshift $\delta(k,L)$ on momentum k and box size L. The interaction energies

* aalexan@gwu.edu
† fxlee@gwu.edu

can be computed on different boxes, thus allowing access to the phaseshift via the “Lüscher formula” afforded by Eq. 4. Two comments are in order about the method. 1) In a box, the matching of wavefunctions on the interaction boundary (to obtain the coefficients α_l and β_l) is replaced by the matrix function $\mathcal{M}(k, L)$. The nature of the interaction is encoded in the energies of the two-body states, which is measured through the quark-gluon dynamics of QCD. 2) Even though the energies are obtained in Euclidean time in a finite box, the phaseshift has the same definition and meaning as in infinite volume and Minkowski time. Once the pion mass is brought to the physical point, the phaseshift computed in the box can be directly compared with experiment. The box is simply a device that serves two purposes at once: to allow the interaction energy to be computed in lattice QCD by making the problem finite thus amenable to a numerical approach, and to facilitate the access to the physical phaseshift via the Lüscher method.

III. PHASESHIFT REDUCTION IN THE ELONGATED BOX

The phaseshift formula in Eq. 4 must be adapted to the symmetry imposed by the box. The issue arises because symmetries in the infinite volume are reduced to the symmetries in the box. Internal symmetries like color, flavor, and isospin are not affected. But angular momentum, which is the measure of rotational symmetries, is greatly affected. Specific to the scattering problem in the box, two areas will be impacted; one is the phaseshift formula used to extract the phaseshifts, the other the interpolators used to construct the scattering states. Our focus is on the former; the latter will be addressed separately. The interpolators must transform according to the symmetries in the box, not in the infinite volume. How the symmetry is reduced from the infinite volume to the periodic box and vice versa is a technical but important issue since we compute energies for two-body states in the box. The subject can be treated formally by group theory.

We consider a box elongated in the z-direction as illustrated in Fig. 1. The infinite volume symmetry group for spatial rotations is $SO(3)$ which has an infinite number of elements and irreducible representations (irreps) labeled by angular momentum J. For the elongated box, the symmetry group is called the dihedral (or tetragonal) group D_4 which has 8 elements and 5 irreps. D_4 is a finite subgroup of the rotation group $SO(3)$. To include half-integral angular momentum as required for baryons, its double cover group ${}^2D_4$ is needed which has 16 elements and 7 irreps. (In infinite volume, the double-cover group of $SO(3)$ is $SU(2)$.) For situations where parity is a good quantum number, the full symmetry group of the elongated box must include space inversion (parity). This group, denoted by ${}^2D_{4h}$, has 32 elements and 14 irreps. The full technical details of the ${}^2D_{4h}$ group are given in Appendix A.

In this paper we will be concerned with two-particle states in an elongated box. Our goal is to derive the relevant Lüscher formulas for the irreps of ${}^2D_{4h}$ corresponding to meson-baryon states, where the meson is spinless and the baryon has spin 1/2. As a cross-check, we also derive the relevant Lüscher formulas for scattering of spinless mesons.

In general, the total angular momentum for scattering two particles with spin S_1 and S_2 is

$$\boldsymbol{J} = \boldsymbol{S}_1 + \boldsymbol{S}_2 + \boldsymbol{l}\,, \tag{5}$$

where l is the relative orbital angular momentum (partial-waves). For the asymptotic states, when the particles are far away from each other, they are not interacting and we can label the states according to S_i and $(S_i)_z$, or equivalently with S, S_i, and S_z, where $\boldsymbol{S} = \boldsymbol{S}_1 + \boldsymbol{S}_2$ is the total spin. The scattering conserves $\boldsymbol{J}$, but can change both $\boldsymbol{l}$ and $\boldsymbol{S}$. For the cases considered in this paper, one of the particles will be spinless so that total spin is simply the spin of the other particle and the situation simplifies since there are no possible changes in the total spin. Moreover, the orbital angular momentum also remains fixed for our cases: In the case that $S = 0$ we have $l = J$ which is conserved. When $S = 1/2$ for a given J, l can assume two different values. These two channels have different parity and since the parity is conserved the value of l cannot change. Thus for $S = 1/2$ we can use the parity of the state to identify which l corresponds to a given J. As such, in some of the formulas and tables in this paper we will indicate the relevant channel by labeling J and the parity. Some comments on parity are in order here. The total parity of the two particle state is equal to

$$P_{tot} = P_1 P_2 (-1)^l \tag{6}$$

where P_1 and P_2 are the intrinsic parities of the two scattering particles. For simplicity we will assume that the intrinsic parity $P_1 P_2$ is positive. For the other case, the parity assignments indicated in the tables and formulas will simply be reversed.

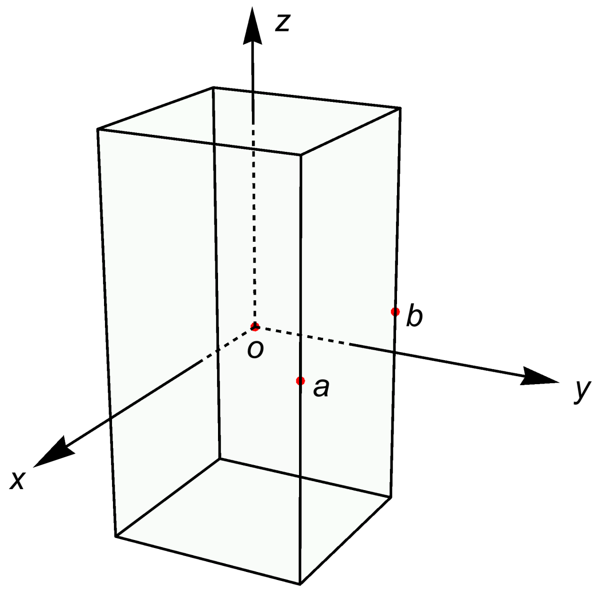

FIG. 1. Symmetry operations that form the dihedral D_4 group in the elongated box whose dimensions are $L \times L \times \eta L$ where η is the elongation factor in the z-direction. The group has 8 elements (rotations that leave the elongated box invariant), which can be divided into 5 conjugacy classes: the identity (I), two $\pi/2$ rotations about the z-axis, one π rotation about the z-axis, two π rotations about x and y axes, and two π rotations about the two diagonals in the xy-plane denoted by Oa and Ob. The operations are performed in a right-hand way with the thumb pointing from the center to the various symmetry points. The full details of the group, with the inclusion of half-integer spin and spatial inversion, are given in Appendix A.

A. Angular momentum in the elongated box

For spherically symmetric interactions the eigenstates of the Hamiltonian in the infinite volume form multiplets that furnish bases for the irreps of $SU(2)$, the double cover of the rotations group. These multiplets are labeled by the angular momentum $J = 0, \frac{1}{2}, 1, \frac{3}{2}, 2, \ldots$. For elongated boxes, these multiplets split into smaller sets that mix under the action of rotations that leave the box invariant, forming the bases for one of the 7 irreps of the ${}^2D_4$ group. Then the question is: for a given J, what irreps are coupled to it? To answer this we have to decompose the irrep J of the full rotation group $SU(2)$, into a direct sum of the irreps of the ${}^2D_4$ group, $J = \bigoplus_i n(\Gamma_i, J)\Gamma_i$, where the coefficient is called the multiplicity, which tells how many times irrep Γ_i appears in the given J. This can be calculated (see for example [11, 12]) using

$$n(\Gamma_i, J) = \frac{1}{g}\sum_k n_k \chi(k, \Gamma_i)\, \chi(\omega_k, J). \tag{7}$$

The index k runs through all 7 classes of ${}^2D_4$ and $g = 16$ is the total number of elements in the group. n_k is the number of elements in the k-th class, and $\chi(k, \Gamma_i)$ are the characters given in Table XI in the appendix. $\chi(\omega_k, J)$ stands for the character of full rotation group for angular momentum J and rotation angle ω_k in class k. This can be computed as follows [13]. Any rotation k is characterized by a rotation axis and the rotation angle ω_k. Since the character (trace) of the matrix is invariant under similarity transformations the result will be equal to an equivalent rotation around the z-axis (the similarity matrix in this case is simply a rotation that takes the rotation axis into the z-axis). The character is then the trace of this diagonal matrix

$$\chi(\omega_k, J) = \sum_{m=-J}^{J} e^{-im\omega_k} = \frac{\sin[(J+1/2)\omega_k]}{\sin(\omega_k/2)}. \tag{8}$$

The results of the decomposition from applying Eq. 7 are given in Table I. Note that limits must be taken if division by zero is encountered in evaluating Eq. 8.

The parity transformation, i, is simply added to ${}^2D_4$ by taking the direct product, ${}^2D_{4h} = {}^2D_4 \otimes \{I, i\}$, so that the irreps are simply doubled each one generating a positive and negative parity irrep. To work out the decomposition of

J	${}^2D_{4h}$	${}^2D_{4h}$	J
0	A_1^+	A_1^+	$0,\, 2,\, 4(2),\, \cdots$
1	$A_2^- \oplus E^-$	A_1^-	$5,\, 7,\, 9(2),\, \cdots$
2	$A_1^+ \oplus B_1^+ \oplus B_2^+ \oplus E^+$	A_2^-	$1,\, 3,\, 5(2),\, \cdots$
3	$A_2^- \oplus B_1^- \oplus B_2^- \oplus 2E^-$	A_2^+	$4,\, 6,\, 8(2),\, \cdots$
4	$2A_1^+ \oplus A_2^+ \oplus B_1^+ \oplus B_2^+ \oplus 2E^+$	B_1^+	$2,\, 4,\, 6(2),\, \cdots$
5	$A_1^- \oplus 2A_2^- \oplus B_1^- \oplus B_2^- \oplus 3E^-$	B_1^-	$3,\, 5,\, 7(2),\, \cdots$
6	$2A_1^+ \oplus A_2^+ \oplus 2B_1^+ \oplus 2B_2^+ \oplus 3E^+$	B_2^+	$2,\, 4,\, 6(2),\, \cdots$
		B_2^-	$3,\, 5,\, 7(2),\, \cdots$
$\cdots$	$\cdots$	E^-	$1,\, 3(2),\, 5(3),\, \cdots$
		E^+	$2,\, 4(2),\, 6(3),\, \cdots$
$1/2$	$G_1^\pm$	$G_1^\pm$	$1/2,\, 3/2,\, 5/2,\, \cdots$
$3/2$	$G_1^\pm \oplus G_2^\pm$	$G_2^\pm$	$3/2,\, 5/2(2),\, 7/2(2),\, \cdots$
$5/2$	$G_1^\pm \oplus 2G_2^\pm$		
$7/2$	$2G_1^\pm \oplus 2G_2^\pm$		
$\cdots$	$\cdots$		

TABLE I. Decomposition of angular momentum in the elongated box according to the irreps of the ${}^2D_{4h}$ group. Both the original reduction (left) and its inverse (right) are shown. Parity is indicated by the plus (even) or minus (odd) sign.

J multiplet into irreps of ${}^2D_{4h}$ we assume that the states have parity $(-1)^l$ ($l = J$ for integer J and $l = J \pm 1/2$ for half-integer cases).

The left part of Table I shows that angular momenta $J = 0$ and $J = 1/2$ correspond to single irreps A_1^+ and $G_1^\pm$, respectively, but it does not mean they have an one-to-one correspondence because the same irrep appears at higher J values, sometimes multiple times in the same J. Then the question is: If an energy eigenstate in the box belongs to one of the irreps, what angular momentum content does it have? In other words, what is the inverse of the correspondence displayed in the left half of the table? If we restrict to $J \leq 9$, the result is shown in the right half of the table. Assuming that the states with higher J-values have higher energy, we see that it is reasonable to identify the ground state in the A_1^+ irrep as $J = 0$, and in $G_1^\pm$ as $J = 1/2$. The ground state of E^- is $J = 1$ if an A_2^- state is also found nearby; or better yet, if they coincide in the infinite volume limit. The interpretation of $G_2^\pm$ as $J = 3/2$ alone is subject to whether $J = 5/2$ or higher have significant contributions. $J = 2$ can be resolved by B_1^+ or B_2^+ or both; $J = 3$ by B_1^- or B_2^- or both. $J = 4$ is accessible by A_2^+ and $J = 5$ is accessible by A_1^-. There is no clean way to resolve higher spins states $J = 5/2$ and $J = 7/2$.

B. Phaseshift formulas in the elongated box

The case for mesons has been considered in Ref. [6]. Here we extend that approach to baryons using our unified treatment of single and double groups in Appendix A. Our starting point is the real part of Eq. 4, expressed for a given total angular momentum J and partial-wave l,

$$\det[\mathcal{M}_{JlM,J'l'M'} - \delta_{JJ'}\delta_{ll'}\delta_{MM'}\cot\delta_{Jl}] = 0\,. \tag{9}$$

The matrix $\mathcal{M}$ is adapted from the original one by Lüscher for integer angular momentum, cubic boxes, and equal masses to the current case of half-integer angular momentum, elongated boxes (limited to z-direction), and unequal masses. The projection to half-integer angular momentum is achieved by a straightforward change of basis by coupling to spin-1/2,

$$\mathcal{M}_{JlM,J'l'M'} = \sum_{mm'm_sm'_s} \big\langle lm, \frac{1}{2}m_s|JM\big\rangle\big\langle l'm', \frac{1}{2}m'_s|J'M'\big\rangle \mathcal{M}_{lm,l'm'}, \tag{10}$$

using Clebsch-Gordan coefficients. The modified matrix for z-elongated box (of elongation η) is

$$\mathcal{M}_{lm,l'm'}(q,\eta) = \sum_{j=|l-l'|}^{l+l'} \sum_{s=-j}^{j} \frac{(-1)^l i^{l+l'}}{\pi^{3/2}\eta q^{j+1}}\, Z_{js}(1,q^2,\eta) \times \langle l0j0|l'0\rangle\langle lmjs|l'm'\rangle \sqrt{\frac{(2l+1)(2j+1)}{(2l'+1)}}. \tag{11}$$

It is customary to introduce the short-hand function for the zeta function,

$$\mathcal{W}_{lm}(1,q^2;\eta) = \frac{\mathcal{Z}_{lm}(1,q^2;\eta)}{\pi^{3/2}\eta q^{l+1}}, \tag{12}$$

so the simplest phaseshift formula reads $\cot\delta = \mathcal{W}_{00}$. The $\mathcal{M}$ matrix is a linear combination of $\mathcal{W}$ functions with purely numerical coefficients. The dimensionless momentum $\boldsymbol{q}$ is defined in terms of the minimal momentum in a periodic box of size L, $\boldsymbol{k} = (2\pi/L)\boldsymbol{q}$. The generalized zeta function for z-elongated boxes is

$$\mathcal{Z}_{lm}(s,q^2;\eta) = \sum_{\boldsymbol{n}\in Z^3} \frac{\mathcal{Y}_{lm}(\widetilde{\boldsymbol{n}})}{(\widetilde{\boldsymbol{n}}^2 - q^2)^s}, \tag{13}$$

where $\mathcal{Y}_{lm}(\boldsymbol{r}) \equiv r^l Y_{lm}(\theta,\phi)$ are homogenous harmonic polynomials and the modified index $\widetilde{\boldsymbol{n}}$ is related to the cubic index $\boldsymbol{n} = (n_x, n_y, n_z)$ by

$$\widetilde{\boldsymbol{n}} = (n_x, n_y, n_z/\eta). \tag{14}$$

Details on how to numerically evaluate the function with elongation can be found in Refs. [6, 9].

The spin-projected matrix $\mathcal{M}_{JlM,J'l'M'}$ is still expressed in terms of angular momentum labels JlM. Our goal is to reduce the matrix to the irreps of the ${}^2D_{4h}$ group in elongated boxes. Operationally, it is equivalent to the reduction of the matrix into its block diagonal form with each block having the dimension of an irrep. This is achieved by another change of basis, using the basis vectors derived in Table XII in Appendix A where the notations used below are fully explained. In the new basis, $\mathcal{M}$ is block-diagonalized by irreps

$$\langle \Gamma\alpha Jln|\mathcal{M}|\Gamma'\alpha' J'l'n'\rangle = \sum_{MM'} \left(C^{\Gamma\alpha n}_{JlM}\right)^* C^{\Gamma'\alpha' n'}_{J'l'M'} \mathcal{M}_{JlM,J'l'M'} = \delta_{\Gamma\Gamma'}\delta_{\alpha\alpha'}\mathcal{M}^{\Gamma}_{Jln,J'l'n'}, \tag{15}$$

where Schur's lemma in linear algebra was used in the second step. For multi-dimensional irreps, the matrix is diagonal in α and the quantization condition does not depend on it. The final form for the phaseshift reduction is

$$\prod_{\Gamma} \det\left[\mathcal{M}^{\Gamma}_{Jln,J'l'n'} - \delta_{JJ'}\delta_{ll'}\delta_{nn'}\cot\delta_{Jl}\right] = 0. \tag{16}$$

If there is no multiplicity, the labels n and n' can be dropped.

Our results for non-zero matrix elements are given in Table II for integral angular momentum up to $J = 4$. We have exploited symmetry properties to simplify the matrix. First, the matrix is hermitian (or symmetric if the elements are real-valued), $\mathcal{M}^{\Gamma}_{Jn,J'n'} = \left(\mathcal{M}^{\Gamma}\right)^*_{J'n',Jn}$, so we only need to display half of the off-diagonal elements. Second, a lot of the $\mathcal{W}$ functions vanish, or satisfy certain constraints, which can be traced back to how the zeta function (more specifically the spherical harmonics) behave under the symmetry operations in the elongated box. The properties are as follows [4, 5].

(i) The standard property $Y_{l-m} = (-1)^m Y^*_{lm}$ translates directly to

$$\mathcal{W}_{l-m} = (-1)^m \mathcal{W}^*_{lm}. \tag{17}$$

(ii) The system is invariant under a mirror reflection about the xy-plane (see Fig. 1). It leads to $Y_{lm}(\theta,\phi) = Y_{lm}(\pi-\theta,\phi) = (-1)^{(l-m)} Y_{lm}(\theta,\phi)$, which means

$$\mathcal{W}_{lm} = 0 \text{ for } l-m = \text{odd. In particular } \mathcal{W}_{l0} = 0 \text{ for } l = 1,3,5,\cdots. \tag{18}$$

It is valid for all systems with inversion symmetry, which leads to a separation into sectors by parity in the table.

(iii) The system is invariant under a $\pi/2$ rotation about the z-axis (or the C_{4z} element of ${}^2D_{4h}$). It leads to the constraint $e^{im\pi/2} = 1$ due to the $e^{im\phi}$ dependence in Y_{lm}. This means

$$\mathcal{W}_{lm} = 0 \text{ for } m \neq 0,4,8,\cdots, \text{ regardless of } l. \tag{19}$$

(iv) The system is invariant under a mirror reflection about the xz-plane, which leads to

$$Y_{lm}(\theta,\phi) = Y_{lm}(\theta, 2\pi-\phi) = Y^*_{lm}(\theta,\phi). \tag{20}$$

This means all the zeta functions are real in the elongated box.

(v) Furthermore, combining conditions (i), (iii), (iv) yields a new condition

$$\mathcal{W}_{l-m} = \mathcal{W}_{lm} \text{ for } m = 0, 4, 8, \cdots , \tag{21}$$

that is, there is no difference between m and $-m$ for the allowed values of m in the elongated box.

Our results agree with those in Ref. [6]. For half-integral angular momentum up to $J = 7/2$ our results for the two irreps G_1 and G_2 are new and are given in Table III. There is two-fold multiplicity for $J = 7/2$ so the n and n' labels are kept explicit.

The final step is to determine the phaseshift using the matrix elements. The A_1^+ sector couples to $J = 0, 2, 4$ with two-fold multiplicity in $J = 4$. The full treatment will lead to a 4×4 matrix in $\mathcal{M}_{Jn,J'n'}$. If the mixing with $J = 4$ can be ignored, we expect only a 2×2 matrix $\mathcal{M}_{JJ'}$ (the multiplicity label is suppressed) and Eq. 16 takes the simple form,

$$\begin{vmatrix} \mathcal{M}_{00} - \cot\delta_0 & \mathcal{M}_{02} \\ \mathcal{M}_{20} & \mathcal{M}_{22} - \cot\delta_2 \end{vmatrix} = 0. \tag{22}$$

The solution is

$$\boldsymbol{A}_1^+ \ \text{ sector}: \quad \cot\delta_0 = \mathcal{W}_{00} + \frac{\mathcal{W}_{20}^2}{\cot\delta_2 - (\mathcal{W}_{00} + \frac{2\sqrt{5}}{7}\mathcal{W}_{20} + \frac{6}{7}\mathcal{W}_{40})}. \tag{23}$$

So the determination of δ_0 generally involves $\mathcal{W}_{00}$, $\mathcal{W}_{20}$, and $\mathcal{W}_{40}$, as well as knowledge of the δ_2. If the coupling to $J = 2$ and higher can be ignored, one gets the simple formula for the $J = 0$ phaseshift $\cot\delta_0 = \mathcal{W}_{00}$. This is the only irrep that has access to the $J = 0$ resonance in the elongated box.

The A_2^- sector at the given cutoff couples to $J = 1, 3$ with no multiplicities. The δ_1 can be determined via

$$\cot\delta_1 = \mathcal{M}_{11} + \frac{\mathcal{M}_{13}\mathcal{M}_{31}}{\cot\delta_3 - \mathcal{M}_{33}} \tag{24}$$

which involves $\mathcal{W}_{l0}$ with $l = 0, 2, 4, 6$ and δ_3. If the coupling to $J = 3$ and higher can be ignored, one gets the simple formula for the $J = 1$ phaseshift

$$\boldsymbol{A}_2^- \ \text{ sector}: \quad \cot\delta_1 = \mathcal{W}_{00} + \frac{2}{\sqrt{5}}\mathcal{W}_{20} \tag{25}$$

which has been used in Ref. [9, 10].

As an example of how to treat multiplicity, we write down the full 3×3 matrix equation in the E^- sector

$$\begin{vmatrix} \mathcal{M}_{11,11} - \cot\delta_1 & \mathcal{M}_{11,31} & 0 \\ \mathcal{M}_{31,11} & \mathcal{M}_{31,31} - \cot\delta_3 & 0 \\ 0 & 0 & \mathcal{M}_{32,32} - \cot\delta_3 \end{vmatrix} = 0. \tag{26}$$

It yields the solution

$$\cot\delta_1 = \mathcal{M}_{11,11} + \frac{\mathcal{M}_{11,31}\mathcal{M}_{31,11}}{\cot\delta_3 - \mathcal{M}_{31,31}}; \quad \cot\delta_3 = \mathcal{M}_{32,32}. \tag{27}$$

Furthermore, if the $J = 3$ state can be ignored, we get the simple formula

$$\boldsymbol{E}^- \ \text{ sector}: \quad \cot\delta_1 = \mathcal{W}_{00} - \frac{1}{\sqrt{5}}\mathcal{W}_{20}. \tag{28}$$

Because of zero coupling between Jn combinations 31 and 32, we get clean access to δ_3 in this sector up to the cutoff $J = 4$,

$$\boldsymbol{E}^- \ \text{ sector}: \quad \cot\delta_3 = \mathcal{W}_{00} - \frac{\sqrt{5}}{3}\mathcal{W}_{20} + \frac{3}{11}\mathcal{W}_{40} - \frac{5}{33\sqrt{13}}\mathcal{W}_{60}. \tag{29}$$

In similar fashion, the $J = 2$ channel can be accessed though the $B_{1/2}^+$ and E^+ sectors. The $J = 3$ channel can also be accessed though the $B_{1/2}^-$ sectors. The best sector for $J = 4$ is A_2^+ where $J = 4$ is the ground state.

Γ	J	n	J'	n'	$\mathcal{M}^{\Gamma}_{Jn,J'n'}$
A_1^+	0	1	0	1	$\mathcal{W}_{00}$
	0	1	2	1	$-\mathcal{W}_{20}$
	0	1	4	1	$\mathcal{W}_{40}$
	0	1	4	2	$\sqrt{2}\mathcal{W}_{44}$
	2	1	2	1	$\mathcal{W}_{00} + \frac{2\sqrt{5}}{7}\mathcal{W}_{20} + \frac{6}{7}\mathcal{W}_{40}$
	2	1	4	1	$-\frac{6}{7}\mathcal{W}_{20} - \frac{20\sqrt{5}}{77}\mathcal{W}_{40} - \frac{15}{11}\sqrt{\frac{5}{13}}\mathcal{W}_{60}$
	2	1	4	2	$\frac{4\sqrt{10}}{11}\mathcal{W}_{44} - \frac{15}{11}\sqrt{\frac{2}{13}}\mathcal{W}_{64}$
	4	1	4	1	$\mathcal{W}_{00} + \frac{20\sqrt{5}}{77}\mathcal{W}_{20} + \frac{486}{1001}\mathcal{W}_{40} + \frac{20}{11\sqrt{13}}\mathcal{W}_{60} + \frac{490}{143\sqrt{13}}\mathcal{W}_{80}$
	4	1	4	2	$\frac{54\sqrt{2}}{143}\mathcal{W}_{44} - \frac{12}{11}\sqrt{\frac{10}{13}}\mathcal{W}_{64} + \frac{21}{13}\sqrt{\frac{10}{187}}\mathcal{W}_{84}$
	4	2	4	2	$\mathcal{W}_{00} - \frac{4\sqrt{5}}{11}\mathcal{W}_{20} + \frac{54}{143}\mathcal{W}_{40} - \frac{4}{11\sqrt{13}}\mathcal{W}_{60} + \frac{7}{143\sqrt{17}}\mathcal{W}_{80} + 21\sqrt{\frac{10}{2431}}\mathcal{W}_{88}$
A_2^-	1	1	1	1	$\mathcal{W}_{00} + \frac{2}{\sqrt{5}}\mathcal{W}_{20}$
	1	1	3	1	$-3\sqrt{\frac{3}{35}}\mathcal{W}_{20} - \frac{4}{\sqrt{21}}\mathcal{W}_{40}$
	3	1	3	1	$\mathcal{W}_{00} + \frac{4}{3\sqrt{5}}\mathcal{W}_{20} + \frac{6}{11}\mathcal{W}_{40} + \frac{100}{33\sqrt{13}}\mathcal{W}_{60}$
A_2^+	4	1	4	1	$\mathcal{W}_{00} - \frac{4\sqrt{5}}{11}\mathcal{W}_{20} + \frac{54}{143}\mathcal{W}_{40} - \frac{4}{11\sqrt{13}}\mathcal{W}_{60} + \frac{7}{143\sqrt{17}}\mathcal{W}_{80} - 21\sqrt{\frac{10}{2431}}\mathcal{W}_{88}$
$B_{1/2}^+$	2	1	2	1	$\mathcal{W}_{00} - \frac{2\sqrt{5}}{7}\mathcal{W}_{20} + \frac{1}{7}\mathcal{W}_{40} \pm \sqrt{\frac{10}{7}}\mathcal{W}_{44}$
	2	1	4	1	$-\frac{\sqrt{15}}{7}\mathcal{W}_{20} + \frac{30\sqrt{3}}{77}\mathcal{W}_{40} - \frac{5}{11}\sqrt{\frac{3}{13}}\mathcal{W}_{60} \pm \frac{2}{11}\sqrt{\frac{30}{7}}\mathcal{W}_{44} \mp \frac{5}{11}\sqrt{\frac{42}{13}}\mathcal{W}_{64}$
	4	1	4	1	$\mathcal{W}_{00} + \frac{8\sqrt{5}}{77}\mathcal{W}_{20} - \frac{27}{91}\mathcal{W}_{40} - \frac{2}{\sqrt{13}}\mathcal{W}_{60} + \frac{196}{143\sqrt{17}}\mathcal{W}_{80}$
					$\pm\frac{81}{143}\sqrt{\frac{10}{7}}\mathcal{W}_{44} \pm \frac{6}{11}\sqrt{\frac{14}{13}}\mathcal{W}_{64} \pm \frac{42}{13}\sqrt{\frac{14}{187}}\mathcal{W}_{84}$
$B_{1/2}^-$	3	1	3	1	$\mathcal{W}_{00} - \frac{7}{11}\mathcal{W}_{40} + \frac{10}{11\sqrt{13}}\mathcal{W}_{60} \mp \frac{\sqrt{70}}{11}\mathcal{W}_{44} \mp \frac{10}{11}\sqrt{\frac{14}{13}}\mathcal{W}_{64}$
E^-	1	1	1	1	$\mathcal{W}_{00} - \frac{1}{\sqrt{5}}\mathcal{W}_{20}$
	1	1	3	1	$-3\sqrt{\frac{2}{35}}\mathcal{W}_{20} + \sqrt{\frac{2}{7}}\mathcal{W}_{40}$
	3	1	3	1	$\mathcal{W}_{00} + \frac{1}{\sqrt{5}}\mathcal{W}_{20} + \frac{1}{11}\mathcal{W}_{40} - \frac{25}{11\sqrt{13}}\mathcal{W}_{60}$
	3	2	3	2	$\mathcal{W}_{00} - \frac{\sqrt{5}}{3}\mathcal{W}_{20} + \frac{3}{11}\mathcal{W}_{40} - \frac{5}{33\sqrt{13}}\mathcal{W}_{60}$
E^+	2	1	2	1	$\mathcal{W}_{00} + \frac{\sqrt{5}}{7}\mathcal{W}_{20} - \frac{4}{7}\mathcal{W}_{40}$
	2	1	4	1	$-\frac{\sqrt{30}}{7}\mathcal{W}_{20} - \frac{5\sqrt{6}}{77}\mathcal{W}_{40} + \frac{10}{11}\sqrt{\frac{6}{13}}\mathcal{W}_{60}$
	4	1	4	1	$\mathcal{W}_{00} + \frac{17\sqrt{5}}{77}\mathcal{W}_{20} + \frac{243}{1001}\mathcal{W}_{40} - \frac{1}{11\sqrt{13}}\mathcal{W}_{60} - \frac{392}{143\sqrt{17}}\mathcal{W}_{80}$
	4	2	4	2	$\mathcal{W}_{00} - \frac{4\sqrt{5}}{11}\mathcal{W}_{20} + \frac{54}{143}\mathcal{W}_{40} - \frac{4}{11\sqrt{13}}\mathcal{W}_{60} + \frac{7}{143\sqrt{17}}\mathcal{W}_{80}$

TABLE II. Non-zero reduced matrix elements in the elongated box (D_{4h} symmetry group) for integral angular momentum up to $J = 4$. The B_1 and B_2 irreps are combined as indicated by the upper/lower signs. The matrix is symmetric in J and J' in each irrep-parity sector. The results are separated according to parity $(-1)^l$.

Γ	J	n	J'	n'	$\mathcal{M}^{\Gamma}_{Jln,J'l'n'}$
$G_1^{\pm}$	$\frac{1}{2}$	1	$\frac{1}{2}$	1	$\mathcal{W}_{00}$
	$\frac{1}{2}$	1	$\frac{3}{2}$	1	$\pm\sqrt{\frac{2}{5}}\mathcal{W}_{20}$
	$\frac{1}{2}$	1	$\frac{5}{2}$	1	$-\sqrt{\frac{3}{5}}\mathcal{W}_{20}$
	$\frac{1}{2}$	1	$\frac{7}{2}$	1	$-\frac{2}{3}\mathcal{W}_{40}$
	$\frac{1}{2}$	1	$\frac{7}{2}$	2	$\mp\frac{2}{3}\sqrt{2}\mathcal{W}_{44}$
	$\frac{3}{2}$	1	$\frac{3}{2}$	1	$\mathcal{W}_{00}+\frac{1}{\sqrt{5}}\mathcal{W}_{20}$
	$\frac{3}{2}$	1	$\frac{5}{2}$	1	$\mp\frac{1}{7}\sqrt{\frac{6}{5}}\mathcal{W}_{20}\mp\frac{2\sqrt{6}}{7}\mathcal{W}_{40}$
	$\frac{3}{2}$	1	$\frac{7}{2}$	1	$-\frac{9}{7}\sqrt{\frac{2}{5}}\mathcal{W}_{20}-\frac{5\sqrt{2}}{21}\mathcal{W}_{40}$
	$\frac{3}{2}$	1	$\frac{7}{2}$	2	$\frac{2}{3}\mathcal{W}_{44}$
	$\frac{5}{2}$	1	$\frac{5}{2}$	1	$\mathcal{W}_{00}+\frac{8}{7\sqrt{5}}\mathcal{W}_{20}+\frac{2}{7}\mathcal{W}_{40}$
	$\frac{5}{2}$	1	$\frac{7}{2}$	1	$\pm\frac{2}{7\sqrt{15}}\mathcal{W}_{20}\pm\frac{10\sqrt{3}}{77}\mathcal{W}_{40}\pm\frac{50}{11\sqrt{39}}\mathcal{W}_{60}$
	$\frac{5}{2}$	1	$\frac{7}{2}$	2	$\mp\frac{2\sqrt{6}}{11}\mathcal{W}_{44}\pm\frac{10}{11}\sqrt{\frac{10}{39}}\mathcal{W}_{64}$
	$\frac{7}{2}$	1	$\frac{7}{2}$	1	$\mathcal{W}_{00}+\frac{5}{21}\sqrt{5}\mathcal{W}_{20}+\frac{27}{77}\mathcal{W}_{40}+\frac{25\mathcal{W}_{60}}{33\sqrt{13}}$
	$\frac{7}{2}$	1	$\frac{7}{2}$	2	$\frac{3\sqrt{2}}{11}\mathcal{W}_{44}-\frac{5}{11}\sqrt{\frac{10}{13}}\mathcal{W}_{64}$
	$\frac{7}{2}$	2	$\frac{7}{2}$	2	$\mathcal{W}_{00}-\frac{\sqrt{5}}{3}\mathcal{W}_{20}+\frac{3}{11}\mathcal{W}_{40}-\frac{5}{33\sqrt{13}}\mathcal{W}_{60}$
$G_2^{\pm}$	$\frac{3}{2}$	1	$\frac{3}{2}$	1	$\mathcal{W}_{00}-\frac{1}{\sqrt{5}}\mathcal{W}_{20}$
	$\frac{3}{2}$	1	$\frac{5}{2}$	1	$\pm\frac{6}{7\sqrt{5}}\mathcal{W}_{20}\mp\frac{2}{7}\mathcal{W}_{40}$
	$\frac{3}{2}$	1	$\frac{5}{2}$	2	$\mp2\sqrt{\frac{2}{7}}\mathcal{W}_{44}$
	$\frac{3}{2}$	1	$\frac{7}{2}$	1	$-\frac{3\sqrt{2}}{7}\mathcal{W}_{20}+\frac{\sqrt{10}}{7}\mathcal{W}_{40}$
	$\frac{3}{2}$	1	$\frac{7}{2}$	2	$\frac{2}{\sqrt{21}}\mathcal{W}_{44}$
	$\frac{5}{2}$	1	$\frac{5}{2}$	1	$\mathcal{W}_{00}+\frac{2}{7\sqrt{5}}\mathcal{W}_{20}-\frac{3}{7}\mathcal{W}_{40}$
	$\frac{5}{2}$	1	$\frac{5}{2}$	2	$\sqrt{\frac{2}{7}}\mathcal{W}_{44}$
	$\frac{5}{2}$	2	$\frac{5}{2}$	2	$\mathcal{W}_{00}-\frac{2\sqrt{5}}{7}\mathcal{W}_{20}+\frac{1}{7}\mathcal{W}_{40}$
	$\frac{5}{2}$	1	$\frac{7}{2}$	1	$\pm\frac{\sqrt{2}}{7}\mathcal{W}_{20}\pm\frac{8\sqrt{10}}{77}\mathcal{W}_{40}\mp\frac{5}{11}\sqrt{\frac{10}{13}}\mathcal{W}_{60}$
	$\frac{5}{2}$	1	$\frac{7}{2}$	2	$\mp\frac{8}{11}\sqrt{\frac{3}{7}}\mathcal{W}_{44}\mp\frac{10}{11}\sqrt{\frac{35}{39}}\mathcal{W}_{64}$
	$\frac{5}{2}$	2	$\frac{7}{2}$	1	$\pm\frac{4}{11}\sqrt{\frac{5}{7}}\mathcal{W}_{44}\mp\frac{10}{11}\sqrt{\frac{7}{13}}\mathcal{W}_{64}$
	$\frac{5}{2}$	2	$\frac{7}{2}$	2	$\mp\frac{1}{7}\sqrt{\frac{10}{3}}\mathcal{W}_{20}\pm\frac{10}{77}\sqrt{6}\mathcal{W}_{40}\mp\frac{5}{11}\sqrt{\frac{2}{39}}\mathcal{W}_{60}$
	$\frac{7}{2}$	1	$\frac{7}{2}$	1	$\mathcal{W}_{00}+\frac{\sqrt{5}}{7}\mathcal{W}_{20}-\frac{9}{77}\mathcal{W}_{40}-\frac{15}{11\sqrt{13}}\mathcal{W}_{60}$
	$\frac{7}{2}$	1	$\frac{7}{2}$	2	$\frac{3}{11}\sqrt{\frac{30}{7}}\mathcal{W}_{44}+\frac{5}{11}\sqrt{\frac{14}{39}}\mathcal{W}_{64}$
	$\frac{7}{2}$	2	$\frac{7}{2}$	2	$\mathcal{W}_{00}-\frac{\sqrt{5}}{21}\mathcal{W}_{20}-\frac{39}{77}\mathcal{W}_{40}+\frac{25}{33\sqrt{13}}\mathcal{W}_{60}$

TABLE III. Non-zero reduced matrix elements in the elongated box ($^2D_{4h}$ symmetry group) for half-integral angular momentum up to $J=7/2$. The even/odd parity sectors are indicated by the upper/lower signs. The matrix is symmetric in Jn and $J'n'$ in each irrep-parity sector.

For half-integral angular momentum, the $G_1^{\pm}$ sector gives the only access to spin-1/2 phaseshifts $\delta_{\frac{1}{2}0}$ (for S_{11}) and $\delta_{\frac{1}{2}1}$ (for P_{11}), assuming a spin-0 meson. However, they mix with $J = 3/2, 5/2, 7/2$ with two-fold multiplicity in $J = 7/2$. The full mixing with cutoff at $J = 7/2$ entails a 5×5 matrix in $\mathcal{M}_{Jn,J'n'}$. The mixing of $J = 1/2$ with $J = 3/2$ and $J = 5/2$ involves $\mathcal{M}_{20}$; while $J = 1/2$ and $J = 7/2$ mixing involves $\mathcal{M}_{40}$ and $\mathcal{M}_{44}$. If we assume coupling to $J = 7/2$ and higher can be ignored, then $\delta_{\frac{1}{2}}$ can be determined via the relation

$$\begin{vmatrix} \mathcal{M}_{\frac{1}{2}\frac{1}{2}} - \cot\delta_{\frac{1}{2}} & \mathcal{M}_{\frac{1}{2}\frac{3}{2}} & \mathcal{M}_{\frac{1}{2}\frac{5}{2}} \\ \mathcal{M}_{\frac{3}{2}\frac{1}{2}} & \mathcal{M}_{\frac{3}{2}\frac{3}{2}} - \cot\delta_{\frac{3}{2}} & \mathcal{M}_{\frac{3}{2}\frac{5}{2}} \\ \mathcal{M}_{\frac{5}{2}\frac{1}{2}} & \mathcal{M}_{\frac{5}{2}\frac{3}{2}} & \mathcal{M}_{\frac{5}{2}\frac{5}{2}} - \cot\delta_{\frac{5}{2}} \end{vmatrix} = 0, \tag{30}$$

where the multiplicity and parity labels are suppressed. The determinant in Eq. 30 involves only the product of the three off-diagonal elements and their squares. Two of them ($\mathcal{M}_{\frac{1}{2}\frac{3}{2}}$ and $\mathcal{M}_{\frac{3}{2}\frac{5}{2}}$) differ by a sign for even/odd parity, and one the same sign ($\mathcal{M}_{\frac{1}{2}\frac{5}{2}}$). This means that Eq. 30 is independent of parity; or $\delta_{\frac{1}{2}0}$ and $\delta_{\frac{1}{2}1}$ obey the same phaseshift formula, so do $\delta_{\frac{3}{2}1}$ and $\delta_{\frac{3}{2}2}$, and $\delta_{\frac{5}{2}2}$ and $\delta_{\frac{5}{2}3}$. So we can suppress the partial-wave l label in δ_{Jl}. In fact, the same conclusion extends to the entire $G_1^{\pm}$ sector. If mixing with only $J = 3/2$ is considered, we have

$$\boldsymbol{G_1^{\pm}} \ \text{sector}: \quad \cot\delta_{\frac{1}{2}} = \mathcal{W}_{00} + \frac{\frac{2}{5}\mathcal{W}_{20}^2}{\cot\delta_{\frac{3}{2}} - (\mathcal{W}_{00} + \frac{1}{\sqrt{5}}\mathcal{W}_{20})}. \tag{31}$$

The determination of spin-1/2 resonances requires $\mathcal{W}_{00}$ and $\mathcal{W}_{20}$ and $\delta_{\frac{3}{2}}$. Only when coupling with $J = 3/2$ can be ignored can one obtain the simplest formula for the Roper ($P11$) and S_{11} phaseshifts $\cot\delta_{\frac{1}{2}} = \mathcal{W}_{00}$. On the other hand, if $\delta_{\frac{1}{2}}$ has been independently determined, Eq.31 can be used to access $\delta_{\frac{3}{2}}$.

In the $G_2^{\pm}$ sector, the leading contribution is $J = 3/2$, followed by $J = 5/2$ and $J = 7/2$ which both have two-fold multiplicity. The full mixing up to $J = 7/2$ also entails a 5×5 matrix in $\mathcal{M}_{Jn,J'n'}$. If we ignore mixing with $J = 7/2$, the phaseshift relation is given by the 3×3 matrix equation,

$$\begin{vmatrix} \mathcal{M}_{\frac{3}{2}1,\frac{3}{2}1} - \cot\delta_{\frac{3}{2}} & \mathcal{M}_{\frac{3}{2}1,\frac{5}{2}1} & \mathcal{M}_{\frac{3}{2}1,\frac{5}{2}2} \\ \mathcal{M}_{\frac{5}{2}2,\frac{3}{2}1} & \mathcal{M}_{\frac{5}{2}1,\frac{5}{2}1} - \cot\delta_{\frac{5}{2}} & 0 \\ \mathcal{M}_{\frac{5}{2}2,\frac{3}{2}1} & 0 & \mathcal{M}_{\frac{5}{2}2,\frac{5}{2}2} - \cot\delta_{\frac{5}{2}} \end{vmatrix} = 0, \tag{32}$$

which has no coupling between the two multiplicities of $J = 5/2$. The solution is

$$\cot\delta_{\frac{3}{2}} = \mathcal{M}_{\frac{3}{2}1,\frac{3}{2}1} + \frac{\mathcal{M}_{\frac{3}{2}1,\frac{5}{2}1}\mathcal{M}_{\frac{3}{2}1,\frac{5}{2}2}}{\cot\delta_{\frac{5}{2}} - \mathcal{M}_{\frac{5}{2}1,\frac{5}{2}1}} + \frac{\mathcal{M}^2_{\frac{5}{2}2,\frac{5}{2}2}}{\cot\delta_{\frac{5}{2}} - \mathcal{M}_{\frac{5}{2}2,\frac{5}{2}2}}. \tag{33}$$

If $J = 5/2$ can be ignored, one gets the simple phaseshift formula

$$\boldsymbol{G_2^{\pm}} \ \text{sector}: \quad \cot\delta_{\frac{3}{2}} = \mathcal{W}_{00} - \frac{1}{\sqrt{5}}\mathcal{W}_{20}. \tag{34}$$

This gives the best access to the Δ resonance in the elongated box. On the other hand, $\delta_{\frac{5}{2}}$ can be extracted in this sector if $\delta_{\frac{3}{2}}$ has been independently determined.

IV. PHASESHIFT REDUCTION IN THE CUBIC BOX

In this section, we revisit the cubic case using the same approach developed in the elongated case. We find such an exercise instructive in at least a couple of ways. First, it can be used to perform consistency checks and validation on the elongated results by comparing with known results. Second, it can serve as a basis for exploring the relationship between the two cases, providing valuable insight into how the results transition from one to the other.

Going from elongated to cubic entails an increase in symmetry. The situation is depicted in Fig. 2. The basic symmetry group is called the octahedral (or cubic) group O which has 24 elements and 5 irreps. The O group is another finite subgroup of the continuum rotation group $SO(3)$. Although the O group is sufficient in describing integral angular momentum in the cubic box, its double-covered group ${}^2O$ is needed for half-integral angular momentum, which has 48 elements and 8 irreps. The full symmetry group in the cubic box must also include space inversion (parity), denoted by ${}^2O_h$, which has 96 elements and 16 irreps. The full technical details of the ${}^2O_h$ group are given in Appendix B.

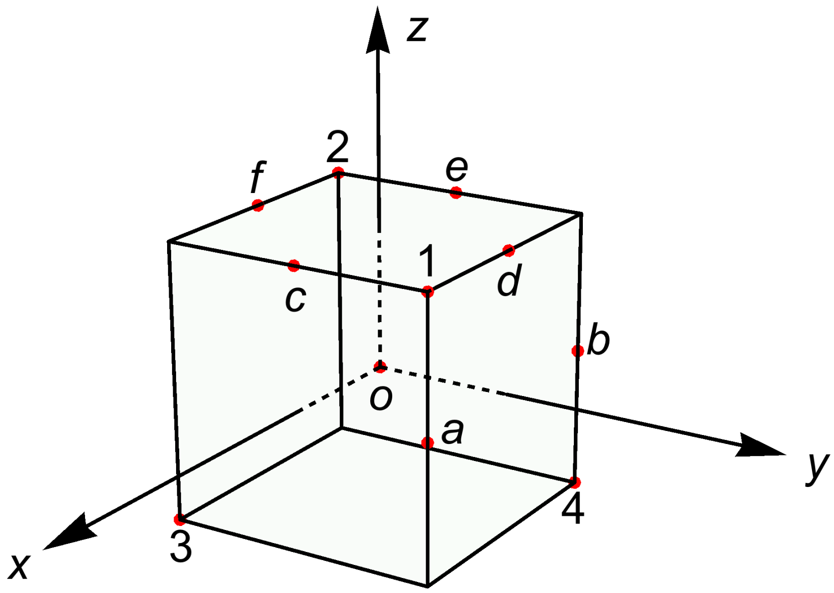

FIG. 2. The 24 symmetry operations in the cubic box that form the octahedral group O. They are divided into 5 conjugacy classes: the identity (I); six $\pi/2$ rotations about the 3 axes; three π rotations about the 3 axes; eight $2\pi/3$ rotations about 4 body diagonals denoted by 1, 2, 3, 4; and six π rotations about axes parallel to 6 face diagonals denoted by a, b, c, d, e, f. The operations are performed in a right-hand way with the thumb pointing from the center to the various symmetry points. The full details of the group, with the inclusion of half-integer spin and spatial inversion, are given in Appendix B.

In the cubic box, instead of the infinite sequence of irreps for $SU(2)$ representing angular momentum (both integer and half-integer) in the infinite volume, only 16 possibilities (the irreps of the ${}^2O_h$ group) exist for angular momentum classification of states. The same decomposition method as in the elongated case, but using the characters in Table XIV in the appendix, leads to Table IV for angular momentum resolution in the cubic box. It shows that angular momenta $J = 0, 1/2, 1, 3/2$ correspond to single irreps. It is safe to identify the ground state in the A_1^+ irrep as $J = 0$, and in $G_1^\pm$ as $J = 1/2$ because the gap to the next contributing J is 3 units away. The identification of the ground state in T_1^- as $J = 1$ would be reasonable as long as no states in the A_2^- and T_2^- irrep are close in energy since this would indicate that they are part of an infinite-volume $J = 3$ multiplet. The ground state of E^+ is $J = 2$ if a T_2^+ state is also found nearby. Likewise, the interpretation of $H^\pm$ as $J = 3/2$ alone is subject to whether $G_2^\pm$ could move in to make $J = 5/2$.

Next we carry out the same phaseshift reduction procedure as in the elongated case, but using the basis vectors for the cubic box given in Table XII in the appendix. The results for the matrix elements are shown in Table V for integral angular momentum, and in Table VI for half-integral angular momentum. Since the cubic case has higher symmetry than the elongated one, there are more symmetry properties on the $\mathcal{W}$ function (or equivalently the zeta function) that can be used to simplify the matrix. More conditions can be found by the general transformation on the zeta function [1],

$$\sum_{m'=-l}^{l} D^{(l)}_{mm'}(R)\mathcal{Z}_{lm'}(s, q^2) = \mathcal{Z}_{lm}(s, q^2), \tag{35}$$

where the Wigner-D functions can be evaluated by using the Euler angles of the cubic group rotations given in Table XIII. In addition to the constraints in the elongated box discussed in Eq. 17 to Eq. 21, we have (up to $l = 8$)

$$\mathcal{W}_{20} = 0,\ \mathcal{W}_{44} = \frac{\sqrt{70}}{14}\mathcal{W}_{40},\ \mathcal{W}_{64} = -\frac{\sqrt{14}}{2}\mathcal{W}_{60},\ \mathcal{W}_{84} = \frac{\sqrt{154}}{33}\mathcal{W}_{80},\ \mathcal{W}_{88} = \frac{\sqrt{1430}}{66}\mathcal{W}_{80}. \tag{36}$$

J	${}^2O_h$	${}^2O_h$	J
0	A_1^+	A_1^+	0, 4, 6, $\cdots$
1	T_1^-	A_1^-	9, 13, 15, $\cdots$
2	$T_2^+ \oplus E^+$	T_1^-	1, 3, 5(2), $\cdots$
3	$A_2^- \oplus T_1^- \oplus T_2^-$	T_1^+	4, 6, 8(2), $\cdots$
4	$A_1^+ \oplus E^+ \oplus T_1^+ \oplus T_2^+$	T_2^+	2, 4, 6(2), $\cdots$
5	$E^- \oplus 2T_1^- \oplus T_2^-$	T_2^-	3, 5, 7(2), $\cdots$
6	$A_1^+ \oplus A_2^+ \oplus E^+ \oplus T_1^+ \oplus 2T_2^+$	E^+	2, 4, 6, $\cdots$
		E^-	5, 7, 9, $\cdots$
$\cdots$	$\cdots$	A_2^-	3, 7, 9, $\cdots$
		A_2^+	6, 10, 12, $\cdots$
1/2	$G_1^\pm$	$G_1^\pm$	1/2, 7/2, 9/2, $\cdots$
3/2	$H^\pm$	$H^\pm$	3/2, 5/2, 7/2, $\cdots$
5/2	$G_2^\pm \oplus H^\pm$	$G_2^\pm$	5/2, 7/2, 11/2, $\cdots$
7/2	$G_1^\pm \oplus G_2^\pm \oplus H^\pm$		
$\cdots$	$\cdots$		

TABLE IV. Decomposition of angular momentum in the cubic box according to the irreps of the ${}^2O_h$ group. Both the original decomposition (left) and its inverse (right) are shown. The number in parentheses indicates the multiplicity of that J in that irrep.

Our results for half-integer angular momentum in Table VI agree with those in Ref. [14], after accounting for the $\sqrt{2l+1}$ factor in the definition of $\mathcal{W}$ functions.

Now we turn to the phaseshift formulas. In the cubic box, the only access to phaseshift δ_0 is in the

$$\boldsymbol{A_1^+} \text{ sector}: \quad \cot\delta_0 = \mathcal{W}_{00}, \tag{37}$$

if we can ignore coupling to $J = 4$ and higher phaseshifts, which are expected to be small at low energies (when $\delta_l(k) \propto k^{2l+1}$).

The only access to phaseshift δ_1 is in the

$$\boldsymbol{T_1^-} \text{ sector}: \quad \cot\delta_1 = \mathcal{W}_{00}, \tag{38}$$

if we can ignore coupling to $J = 3$ and higher. Although the formula for δ_1 is the same as that for δ_0, differences can arising from mixing with higher states, and from operators constructed under the different irreps to access the states.

The δ_2 phaseshift can be accessed either in the

$$\boldsymbol{E^+} \text{ sector}: \quad \cot\delta_2 = \mathcal{W}_{00} + \frac{6}{7}\mathcal{W}_{40}, \tag{39}$$

or in the

$$\boldsymbol{T_2^+} \text{ sector}: \quad \cot\delta_2 = \mathcal{W}_{00} - \frac{4}{7}\mathcal{W}_{40}. \tag{40}$$

Similarly, the best access to δ_3 phaseshift is in the A_2^- sector or T_2^- sector. The best access to δ_4 phaseshift is in the T_1^+ sector.

For half-integer spin, the only access to spin-1/2 resonance phaseshift is in the

$$\boldsymbol{G_1^\pm} \text{ sector}: \quad \cot\delta_{\frac{1}{2}} = \mathcal{W}_{00}. \tag{41}$$

It has a large gap to the next state it mixes with, $J = 7/2$, which involves $\mathcal{W}_{40}$. Note that $\delta_{\frac{1}{2}}$ stands for $\delta_{\frac{1}{2}0}$ for G_1^+, and $\delta_{\frac{1}{2}1}$ for G_1^-. For πN scattering, they correspond to the S_{11} and P_{11} (Roper) phaseshifts, respectively. We see that obey the same formula in the cubic box.

The only access to phaseshift $\delta_{\frac{3}{2}}$ is in the $H^\pm$ sector, with leading contribution

$$\boldsymbol{H^\pm} \text{ sector}: \quad \cot\delta_{\frac{3}{2}} = \mathcal{W}_{00}. \tag{42}$$

This is the best sector to extract the phaseshift of Δ resonance. Mixing with higher states $J = 5/2$ and $J = 7/2$ can be included using the provided matrix elements.

Γ	J	J'	$\mathcal{M}^{\Gamma}_{J,J'}$
A_1^+	0	0	$\mathcal{W}_{00}$
	0	4	$\frac{36}{\sqrt{21}}\mathcal{W}_{40}$
	4	4	$\mathcal{W}_{00} + \frac{108}{143}\mathcal{W}_{40} + \frac{80}{11\sqrt{13}}\mathcal{W}_{60} + \frac{560}{143\sqrt{17}}\mathcal{W}_{80}$
A_2^-	3	3	$\mathcal{W}_{00} - \frac{12}{11}\mathcal{W}_{40} + \frac{80}{11\sqrt{13}}\mathcal{W}_{60}$
E^+	2	2	$\mathcal{W}_{00} + \frac{6}{7}\mathcal{W}_{40}$
	2	4	$-\frac{40\sqrt{3}}{77}\mathcal{W}_{40} - \frac{30}{11}\sqrt{\frac{3}{13}}\mathcal{W}_{60}$
	4	4	$\mathcal{W}_{00} + \frac{108}{1001}\mathcal{W}_{40} - \frac{64}{11\sqrt{13}}\mathcal{W}_{60} + \frac{392}{143\sqrt{17}}\mathcal{W}_{80}$
T_1^-	1	1	$\mathcal{W}_{00}$
	1	3	$-\frac{4}{\sqrt{21}}\mathcal{W}_{40}$
	3	3	$\mathcal{W}_{00} + \frac{6}{11}\mathcal{W}_{40} + \frac{100}{33\sqrt{13}}\mathcal{W}_{60}$
T_1^+	4	4	$\mathcal{W}_{00} + \frac{54}{143}\mathcal{W}_{40} - \frac{4}{11\sqrt{13}}\mathcal{W}_{60} - \frac{448}{143\sqrt{17}}\mathcal{W}_{80}$
T_2^+	2	2	$\mathcal{W}_{00} - \frac{4}{7}\mathcal{W}_{40}$
	2	4	$-\frac{20\sqrt{3}}{77}\mathcal{W}_{40} + \frac{40}{11}\sqrt{\frac{3}{13}}\mathcal{W}_{60}$
	4	4	$\mathcal{W}_{00} - \frac{54}{77}\mathcal{W}_{40} + \frac{20}{11\sqrt{13}}\mathcal{W}_{60}$
T_2^-	3	3	$\mathcal{W}_{00} - \frac{2}{11}\mathcal{W}_{40} - \frac{60}{11\sqrt{13}}\mathcal{W}_{60}$

TABLE V. Non-zero reduced matrix elements in the cubic box for integral angular momentum up to $J = 4$ (symmetry group O_h). The matrix is symmetric in J and J' in each irrep-parity sector.

The best access to $\delta_{\frac{5}{2}}$ phaseshift is in the

$$\boldsymbol{G}_2^{\pm} \text{ sector}: \quad \cot\delta_{\frac{5}{2}} = \mathcal{W}_{00} - \frac{4}{7}\mathcal{W}_{40}. \tag{43}$$

It couples with $J = 7/2$ and higher states. The combined results from the different sectors can help isolate the phaseshifts for low-lying baryon resonances in πN scattering in the cubic box.

V. RELATIONS BETWEEN THE CUBIC AND ELONGATED CASES

Having derived the phaseshift formulas in both the cubic and elongated boxes, we would like to explore the relationship between the two. Going from cubic box to elongated box, the symmetry is reduced. The two have different irreps: $A_1^{\pm}, A_2^{\pm}, E^{\pm}, T_1^{\pm}, T_2^{\pm}, G_1^{\pm}, G_2^{\pm}, H^{\pm}$ with respective dimensionality $1, 1, 2, 3, 3, 2, 2, 4$ in the cubic box, and $A_1^{\pm}, A_2^{\pm}, E^{\pm}, B_1^{\pm}, B_2^{\pm}, G_1^{\pm}, G_2^{\pm}$ with respective dimensionality $1, 1, 2, 1, 1, 2, 2$ in the elongated box. How do they transition to one another? The descent in symmetry follows the so-called subduction rules in group theory (see, for example, Ref. [15]), shown in Table VII. In the same table, the rules for ${}^2C_{4v}$ are also given. They are relevant for states with non-zero momentum, to be discussed in the next section.

Specifically, we want to explore the relationships manifested in the matrix elements $\mathcal{M}^{\Gamma}_{Jln,J'l'n'}$ for phaseshifts. In the case of integer angular momentum, we find the following correspondence by comparing the matrix elements in Table V and Table II. In the following, the cubic elements are on the left-hand side, the elongated on the right-hand side.

(i) For $(J, J') = (0, 0)$, the A_1 has one-to-one correspondence

$$\mathcal{M}^{A_1^+}_{00} = \mathcal{M}^{A_1^+}_{00}. \tag{44}$$

Γ	J	J'	$\mathcal{M}^{\Gamma}_{Jl,J'l'}$
$G_1^{\pm}$	$\frac{1}{2}$	$\frac{1}{2}$	$\mathcal{W}_{00}$
	$\frac{1}{2}$	$\frac{7}{2}$	$\mp\frac{4}{\sqrt{21}}\mathcal{W}_{40}$
	$\frac{7}{2}$	$\frac{7}{2}$	$\mathcal{W}_{00}+\frac{6}{11}\mathcal{W}_{40}+\frac{100}{33\sqrt{13}}\mathcal{W}_{60}$
$G_2^{\pm}$	$\frac{5}{2}$	$\frac{5}{2}$	$\mathcal{W}_{00}-\frac{4}{7}\mathcal{W}_{40}$
	$\frac{5}{2}$	$\frac{7}{2}$	$\pm\frac{20\sqrt{3}}{77}\mathcal{W}_{40}\mp\frac{40}{11}\sqrt{\frac{3}{13}}\mathcal{W}_{60}$
	$\frac{7}{2}$	$\frac{7}{2}$	$\mathcal{W}_{00}-\frac{54}{77}\mathcal{W}_{40}+\frac{20}{11\sqrt{13}}\mathcal{W}_{60}$
$H^{\pm}$	$\frac{3}{2}$	$\frac{3}{2}$	$\mathcal{W}_{00}$
	$\frac{3}{2}$	$\frac{5}{2}$	$\mp\frac{2\sqrt{6}}{7}\mathcal{W}_{40}$
	$\frac{3}{2}$	$\frac{7}{2}$	$\frac{2}{7}\sqrt{\frac{10}{3}}\mathcal{W}_{40}$
	$\frac{5}{2}$	$\frac{5}{2}$	$\mathcal{W}_{00}+\frac{2}{7}\mathcal{W}_{40}$
	$\frac{5}{2}$	$\frac{7}{2}$	$\mp\frac{12\sqrt{5}}{77}\mathcal{W}_{40}\mp\frac{20}{11}\sqrt{\frac{5}{13}}\mathcal{W}_{60}$
	$\frac{7}{2}$	$\frac{7}{2}$	$\mathcal{W}_{00}+\frac{6}{77}\mathcal{W}_{40}-\frac{80}{33\sqrt{13}}\mathcal{W}_{60}$

TABLE VI. Non-zero reduced matrix elements in the cubic box for half-integral angular momentum up to $J = 7/2$ (symmetry group ${}^2O_h$). The even/odd parity sectors are indicated by the upper/lower signs. The matrix is symmetric in Jl and $J'l'$ in each irrep sector.

${}^2O_h$	A_1^+	A_2^+	E^+	T_1^+	T_2^+	G_1^+	G_2^+	H^+	A_1^-	A_2^-	E^-	T_1^-	T_2^-	G_1^-	G_2^-	H^-
${}^2D_{4h}$	A_1^+	B_1^+	$A_1^+\oplus B_1^+$	$A_2^+\oplus E^+$	$B_2^+\oplus E^+$	G_1^+	G_2^+	$G_1^+\oplus G_2^+$	A_1^-	B_1^-	$A_1^-\oplus B_1^-$	$A_2^-\oplus E^-$	$B_2^-\oplus E^-$	G_1^-	G_2^-	$G_1^-\oplus G_2^-$
${}^2C_{4v}$	A_1	B_1	$A_1\oplus B_1$	$A_2\oplus E$	$B_2\oplus E$	G_1	G_2	$G_1\oplus G_2$	A_2	B_2	$A_2\oplus B_2$	$A_1\oplus E$	$B_1\oplus E$	G_1	G_2	$G_1\oplus G_2$

TABLE VII. Subduction rules in the descent in symmetry in the group chain from the cubic box (${}^2O_h$), to the elongated box (${}^2D_{4h}$), to moving frame (${}^2C_{4v}$).

(ii) For $(J, J') = (1, 1)$, T_1^- splits into A_2^- and E^- according to

$$\mathcal{M}_{11}^{T_1^-} = \frac{1}{3}\mathcal{M}_{11}^{A_2^-} + \frac{2}{3}\mathcal{M}_{11}^{E^-}. \tag{45}$$

The factors are related to the fact that T_1 is a three-dimensional irrep, whereas A_2 one-dimensional and E two-dimensional. Going from the elongated to the cubic symmetry, even though the matrix elements $\mathcal{M}_{11}^{A_2^-}$ and $\mathcal{M}_{11}^{E^-}$ will individually go to $\mathcal{M}_{11}^{T_1^-} = \mathcal{W}_{00}$ in the limit $\eta \to 1$ because $\mathcal{W}_{20}$ goes to zero in the same limit, Eq. 45 shows how to follow this limit by subduction rule in this particular channel. If coupling to $J = 3$ and higher can be ignored, this relationship translates directly into one for the phaseshift:

$$\cot\delta_1(\mathcal{T}_1^-) = \frac{1}{3}\cot\delta_1(A_2^-) + \frac{2}{3}\cot\delta_1(E^-). \tag{46}$$

(iii) For $(J, J') = (2, 2)$, there are two scenarios. The first is that E^+ splits into A_1^+ and B_1^+ according to

$$\mathcal{M}_{22}^{E^+} = \frac{1}{2}(\mathcal{M}_{22}^{A_1^+} + \mathcal{M}_{22}^{B_1^+}). \tag{47}$$

The second is that T_2^+ splits into B_2^+ and E^+ according to

$$\mathcal{M}_{22}^{T_1^-} = \frac{1}{3}\mathcal{M}_{22}^{B_2^+} + \frac{2}{3}\mathcal{M}_{22}^{E^+}. \tag{48}$$

In both cases, the condition $\mathcal{W}_{44} = \frac{\sqrt{70}}{14}\mathcal{W}_{40}$ in the cubic box has been used.

Relations for other JJ' combinations can be found in similar fashion.

In the case of half-integral angular momentum, we find the following correspondence by comparing the matrix elements in Table VI and Table III.

(i) For $(J, J') = (1/2, 1/2)$, there is one-to-one correspondence

$$\mathcal{M}^{G_1^\pm}_{\frac{1}{2}\frac{1}{2}} = \mathcal{M}^{G_1^\pm}_{\frac{1}{2}\frac{1}{2}}. \tag{49}$$

(ii) For $(J, J') = (3/2, 3/2)$, $H^\pm$ splits into $G_1^\pm$ and $G_2^\pm$ evenly according to

$$\mathcal{M}^{H^\pm}_{\frac{3}{2}\frac{3}{2}} = \frac{1}{2}\left(\mathcal{M}^{G_1^\pm}_{\frac{3}{2}\frac{3}{2}} + \mathcal{M}^{G_2^\pm}_{\frac{3}{2}\frac{3}{2}}\right). \tag{50}$$

The dimensionality also checks out $(4 = 2 \oplus 2)$.

(iii) For $(J, J') = (5/2, 5/2)$, there are two scenarios. The first is $G_2^\pm$ to $G_2^\pm$, but the latter has a two-fold multiplicity labeled by n, n' in the notation $\mathcal{M}^\Gamma_{JJ'}(n, n')$. The specific combination is found to be

$$\mathcal{M}^{G_2^\pm}_{\frac{5}{2}\frac{5}{2}} = \frac{5}{6}\mathcal{M}^{G_2^\pm}_{\frac{5}{2}\frac{5}{2}}(1,1) - \frac{\sqrt{5}}{6}[\mathcal{M}^{G_2^\pm}_{\frac{5}{2}\frac{5}{2}}(1,2) + \mathcal{M}^{G_2^\pm}_{\frac{5}{2}\frac{5}{2}}(2,1)] + \frac{1}{6}\mathcal{M}^{G_2^\pm}_{\frac{5}{2}\frac{5}{2}}(2,2). \tag{51}$$

The second is that $H^\pm$ splits into $G_1^\pm$ and $G_2^\pm$ according to

$$\mathcal{M}^{H^\pm}_{\frac{5}{2}\frac{5}{2}} = \frac{1}{2}\mathcal{M}^{G_1^\pm}_{\frac{5}{2}\frac{5}{2}} + \frac{1}{12}\mathcal{M}^{G_2^\pm}_{\frac{5}{2}\frac{5}{2}}(1,1) + \frac{\sqrt{5}}{12}[\mathcal{M}^{G_2^\pm}_{\frac{5}{2}\frac{5}{2}}(1,2) + \mathcal{M}^{G_2^\pm}_{\frac{5}{2}\frac{5}{2}}(2,1)] + \frac{5}{12}\mathcal{M}^{G_2^\pm}_{\frac{5}{2}\frac{5}{2}}(2,2). \tag{52}$$

Relations for other JJ' combinations can be found in similar fashion.

VI. MOVING STATES IN A CUBIC BOX

So far we have considered two-body states that are at rest; the two particles have back-to-back nonzero momentum, but the total momentum $\boldsymbol{P} = 0$ in the lab frame. Now we consider giving the system a boost. In the center-of-mass frame (CM) the cubic box becomes a parallelepiped, in which the side parallel to the directions of the boost is contracted by the Lorentz boost factor γ, whereas the size in the perpendicular direction is unchanged. The advantage of boosting is that it can lower the center-of-mass energy, thus allowing wider access to the resonance region. The invariant energy of the system is

$$W = \sqrt{m_1^2 + \boldsymbol{k}^2} + \sqrt{m_2^2 + \boldsymbol{k}^2}, \tag{53}$$

where $\boldsymbol{k}$ is the relative momentum in the CM frame. The energy in the lab frame

$$E_{lab} = \sqrt{m_1^2 + \boldsymbol{p}_1^2} + \sqrt{m_2^2 + \boldsymbol{p}_2^2}, \tag{54}$$

is the same as W when the system is at rest. But when the system is moving with momentum

$$\boldsymbol{P} = \boldsymbol{p}_1 + \boldsymbol{p}_2 = \frac{2\pi}{L}\boldsymbol{d} \tag{55}$$

as measured in the lab frame, the CM energy is lowered according to

$$W = \sqrt{E_{lab}^2 - \boldsymbol{P}^2}. \tag{56}$$

The two energies are related by $W = E_{lab}/\gamma$ where the boost factor γ and boost velocity $\boldsymbol{v}$ are given by

$$\gamma = \frac{1}{\sqrt{1 - \boldsymbol{v}^2}} \text{ with } \boldsymbol{v} = \frac{\boldsymbol{P}}{E_{lab}}. \tag{57}$$

The procedure to extract phaseshift is to first measure the interaction energy E_{lab}, then determine W via the boost factor, then $\boldsymbol{k}$ via Eq. 53, then $\delta(k)$ via the Lüscher formula. Ref. [5] considered boosts in three different directions and Ref. [4] in two different directions. We restrict ourselves to boosts only in the z-direction: $\boldsymbol{d} = (0, 0, d_z)$ with $d_z \in \mathbb{Z}$. These boosts preserve the symmetry of the elongated box, as viewed from the CM frame. The wavefunction for the relative position $\psi(\boldsymbol{r})$ still satisfies the Helmholtz equation, Eq. 1, when the distance between particles is larger than the interaction range, but the boundary conditions are different for boosted states [2–5]:

$$\psi(\boldsymbol{r} + \hat{\gamma}\boldsymbol{n}L) = e^{i\pi A\boldsymbol{n}\cdot\boldsymbol{d}}\psi(\boldsymbol{r})\,, \tag{58}$$

where $\hat{\gamma}\boldsymbol{n} \equiv \gamma\boldsymbol{n}_\parallel + \boldsymbol{n}_\perp$ and

$$A = 1 + \frac{m_1^2 - m_2^2}{W^2}\,. \tag{59}$$

The full symmetry group that preserves these boundary conditions for the case when $\boldsymbol{d}$ is parallel with the z-direction in the cubic box is ${}^2C_{4v}$. We relegate the details for this group to Appendix C. The most important difference from the zero momentum case is that the boundary conditions specified above are not invariant under parity, so the solutions of the Helmholtz equation are a mixture of different parities. For the meson-baryon states, this means that we can no longer identify the orbital angular momentum l for a given J using parity. For the two-meson states, the most important consequence is that the irreps now overlap with all angular momenta J, not just the even (or odd) ones.

When the phaseshift reduction is carried out for boosting using the basis vectors in Table XVI, the matrix elements are obtained in Table VIII for integer J and Table IX for half-integer J. For diagonal JJ' and ll' combinations, the two elements corresponding to the even and odd l are the same, so only one of them is shown. For example, $\mathcal{M}^{\Gamma}_{\frac{1}{2}0,\frac{1}{2}0} = \mathcal{M}^{\Gamma}_{\frac{1}{2}1,\frac{1}{2}1}$, $\mathcal{M}^{\Gamma}_{\frac{3}{2}1,\frac{3}{2}1} = \mathcal{M}^{\Gamma}_{\frac{3}{2}2,\frac{3}{2}2}$, and so on. Notice the appearance of $\mathcal{W}$ functions with odd values of J due to loss of parity. Our results agree fully with those in Ref. [5] in the case of $\boldsymbol{d} = (0, 0, 1)$ for up to $J = 2$ for mesons and up to $J = 3/2$ for baryons, after accounting for the $\sqrt{2l+1}$ factor in the definition of the $\mathcal{W}_{lm}$ functions. Our results extend to $J = 3$ and $J = 5/2$. Our results for integer J in Table VIII also largely agree with those in Ref. [3], except for the missing $\sqrt{3}$ factor in $\mathcal{W}_{10}$ that is also pointed out in Ref. [4]. The agreements give a concrete demonstration that the phaseshift formulas are independent of the basis vectors since we used different basis vectors.

The $\mathcal{W}$ functions in Table VIII and Table IX are the modified versions of the cubic ones to incorporate boosting (indicated by γ and $\boldsymbol{d}$) in the cubic box (no η factor),

$$\mathcal{W}_{lm}(1, q^2, \gamma) = \frac{\mathcal{Z}^{\boldsymbol{d}}_{lm}(1, q^2, \gamma)}{\pi^{\frac{3}{2}}\gamma q^{l+1}}\,. \tag{60}$$

The relevant zeta function is

$$\mathcal{Z}^{\boldsymbol{d}}_{lm}(s, q^2, \gamma) = \sum_{\widetilde{\boldsymbol{n}} \in P_{\boldsymbol{d}}(\gamma)} \frac{\mathcal{Y}_{lm}(\widetilde{\boldsymbol{n}})}{(\widetilde{\boldsymbol{n}}^2 - q^2)^s}, \tag{61}$$

where the summation region changes to

$$P_{\boldsymbol{d}}(\gamma) = \left\{ \widetilde{\boldsymbol{n}} \in \mathbb{R}^3 \mid \widetilde{\boldsymbol{n}} = \hat{\gamma}^{-1}(\boldsymbol{m} + \frac{1}{2}A\,\boldsymbol{d}), \boldsymbol{m} \in \mathbb{Z}^3 \right\}, \tag{62}$$

where $\widetilde{\boldsymbol{n}}$ is over real numbers and $\boldsymbol{m}$ over integers. The projector $\hat{\gamma}^{-1}$ operating on a vector $\boldsymbol{n}$ is defined as only affecting the boost direction

$$\hat{\gamma}^{-1}\boldsymbol{n} = \frac{\boldsymbol{n}_\parallel}{\gamma} + \boldsymbol{n}_\perp \text{ where } \boldsymbol{n}_\parallel = \frac{\boldsymbol{v}(\boldsymbol{n}\cdot\boldsymbol{v})}{\boldsymbol{v}^2} \text{ and } \boldsymbol{n}_\perp = \boldsymbol{n} - \boldsymbol{n}_\parallel. \tag{63}$$

The fact that the two particles have unequal masses enters explicitly in the zeta function through the scaling factor in front of the boost $\boldsymbol{d}$ in Eq. 62 [4, 5], A, which reduces to one when the two masses are equal. For unequal masses, what happens if they are switched? This question can be answered by examining the mass dependence in the zeta function in Eq. 61. Interchanging m_1 and m_2 only affects the A factor in the summation grid in Eq. 62. The result is a change in sign of the set of points to be summed over from $\widetilde{\boldsymbol{n}}$ to $-\widetilde{\boldsymbol{n}}$ (the mirror image grid). This leads to an overall sign change in the zeta function, which does not affect the phaseshift determinants. So the order of m_1 and m_2 does not matter; they have the same phaseshift formula. There is a real physical effect, however, that depends on the order of m_1 and m_2. Let us use an example and assume $m_2 > m_1$. For a given boost $\boldsymbol{d} = (0, 0, 1)$, there are two possible arrangements for momenta in the lab frame: case 1 is $\boldsymbol{p}_1 = (0, 0, 0)$ and $\boldsymbol{p}_2 = (0, 0, 2\pi/L)$, case 2 is $\boldsymbol{p}_1 = (0, 0, 2\pi/L)$

and $\boldsymbol{p}_2 = (0,0,0)$. According to Eq. 54, when the heavier particle (m_2) possesses the nonzero momentum (case 1), the energy E_{lab} is lower than in case 2. It means case 1 has a lower CM energy W, which means a lower CM back-to-back momentum $\boldsymbol{k}$. Another way of looking at it is by Eq. 57: case 1 has higher boost velocity $\boldsymbol{v}$ and boost factor γ, thus lower energy.

In the case of equal masses, parity (or space inversion) is restored, leading to considerable simplifications in Table VIII and Table IX. All the odd l zeta functions vanish. The matrix elements can then be separated into sectors by irrep-parity combinations.

In the absence of a boost ($\boldsymbol{d} = 0$ and $\gamma = 1$), the zeta function returns to the original one in the cubic box. How the cubic symmetry is restored follows the subduction rules between ${}^2O_h$ and ${}^2C_{4v}$ in Table VII, similar to between ${}^2O_h$ and ${}^2D_{4h}$ discussed in the previous section, except the role reversals in A_1 and B_1 and A_2 and B_2 for negativity parity.

VII. MOVING STATES IN AN ELONGATED BOX

Elongation in one of the dimensions picks out a special direction in space; so does boosting. The general situation when the two directions do not align is complicated. However, when the elongation and the boost are in the same direction, such as the z-axis considered in this work, deriving the Lüscher formulas for moving states is considerably simpler.

The key observation is that the ${}^2C_{4v}$ symmetry group for moving states is isomorphic to ${}^2D_4$ of the z-elongated box. Therefore, the matrix elements for the phaseshifts have exactly the same forms as those in Table VIII and Table IX. The only difference is that we need to make a small change in the zeta functions, namely, add the elongation factor η in Equations 60 to 62, so they now read

$$\mathcal{W}_{lm}(1, q^2, \gamma, \eta) = \frac{\mathcal{Z}^{\boldsymbol{d}}_{lm}(1, q^2, \gamma, \eta)}{\pi^{\frac{3}{2}} \eta\gamma q^{l+1}}, \tag{64}$$

and

$$\mathcal{Z}^{\boldsymbol{d}}_{lm}(s, q^2, \gamma, \eta) = \sum_{\tilde{\boldsymbol{n}} \in P_{\boldsymbol{d}}(\gamma,\eta)} \frac{\mathcal{Y}_{lm}(\tilde{\boldsymbol{n}})}{(\tilde{\boldsymbol{n}}^2 - q^2)^s}, \tag{65}$$

where the summation grid changes to

$$P_{\boldsymbol{d}}(\gamma, \eta) = \left\{ \tilde{\boldsymbol{n}} \in \mathbb{R}^3 \mid \tilde{\boldsymbol{n}} = \hat{\gamma}^{-1}\hat{\eta}^{-1}(\boldsymbol{m} + \frac{1}{2}A\,\boldsymbol{d}), \boldsymbol{m} \in \mathbb{Z}^3 \right\}, \tag{66}$$

with the projector $\hat{\eta}^{-1}$ acting on a vector $\boldsymbol{m}$ to mean $\hat{\eta}^{-1}\boldsymbol{m} = (m_x, m_y, m_z/\eta)$. Since the boost and elongation are in the same z-direction, the factors always appear as a product $\gamma\eta$ in the zeta function, facilitating its evaluation.

Due to lack of parity in boosted states, there is mixing between odd and even J and the entire sector for each irrep becomes coupled. This means that the phaseshift formulas are generally more complicated for moving states than for the ones at rest. For example, the A_2 irrep is no longer a good sector for isolating $J = 1$ resonances since $J = 0$ appears below it as the ground state. The E sector still has $J = 1$ as the ground state, but mixes with all states $J = 2$ and higher, as opposed to only odd states $J = 3, 5, \ldots$, as is the case for states at rest. If we only consider coupling with $J = 2$, the phaseshift formula is

$$\begin{vmatrix} \mathcal{W}_{00} - \frac{1}{\sqrt{5}}\mathcal{W}_{20} - \cot\delta_1 & i\sqrt{\frac{3}{5}}\mathcal{W}_{10} - \frac{3i}{\sqrt{35}}\mathcal{W}_{30} \\ -i\sqrt{\frac{3}{5}}\mathcal{W}_{10} + \frac{3i}{\sqrt{35}}\mathcal{W}_{30} & \mathcal{W}_{00} + \frac{\sqrt{5}}{7}\mathcal{W}_{20} - \frac{4}{7}\mathcal{W}_{40} - \cot\delta_2 \end{vmatrix} = 0. \tag{67}$$

This formula applies to processes such as $\pi K \to K^*$, and $\pi\rho \to a_1$ (S-wave only).

In the G_1 sector, the channels $\delta_{\frac{1}{2}0}$ (S_{11} resonance for π-N scattering) and $\delta_{\frac{1}{2}1}$ (P_{11} or Roper resonance) become coupled,

$$\begin{vmatrix} \mathcal{W}_{00} - \cot\delta_{\frac{1}{2}0} & -\frac{i}{\sqrt{3}}\mathcal{W}_{10} \\ \frac{i}{\sqrt{3}}\mathcal{W}_{10} & \mathcal{W}_{00} - \cot\delta_{\frac{1}{2}1} \end{vmatrix} = 0, \tag{68}$$

if we ignore mixing with higher J. So the determination of spin-1/2 resonances requires $\mathcal{W}_{10}$ in addition to $\mathcal{W}_{00}$ at the leading order. The two phaseshifts have to be extracted simultaneously.

Γ	J	n	J'	n'	$\mathcal{M}^{\Gamma}_{Jn,J'n'}$
A_1	0	1	0	1	$\mathcal{W}_{00}$
	0	1	1	1	$i\mathcal{W}_{10}$
	0	1	2	1	$-\mathcal{W}_{20}$
	0	1	3	1	$-i\mathcal{W}_{30}$
	1	1	1	1	$\mathcal{W}_{00}+\frac{2}{\sqrt{5}}\mathcal{W}_{20}$
	1	1	2	1	$\frac{2i}{\sqrt{5}}\mathcal{W}_{10}+3i\sqrt{\frac{3}{35}}\mathcal{W}_{30}$
	1	1	3	1	$-3\sqrt{\frac{3}{35}}\mathcal{W}_{20}-\frac{4}{\sqrt{21}}\mathcal{W}_{40}$
	2	1	2	1	$\mathcal{W}_{00}+\frac{2\sqrt{5}}{7}\mathcal{W}_{20}+\frac{6}{7}\mathcal{W}_{40}$
	2	1	3	1	$3i\sqrt{\frac{3}{35}}\mathcal{W}_{10}+\frac{4i}{3\sqrt{5}}\mathcal{W}_{30}+\frac{10}{3}i\sqrt{\frac{5}{77}}\mathcal{W}_{50}$
	3	1	3	1	$\mathcal{W}_{00}+\frac{4}{3\sqrt{5}}\mathcal{W}_{20}+\frac{6}{11}\mathcal{W}_{40}+\frac{100}{33\sqrt{13}}\mathcal{W}_{60}$
$B_{1/2}$	2	1	2	1	$\mathcal{W}_{00}-\frac{2\sqrt{5}}{7}\mathcal{W}_{20}+\frac{1}{7}\mathcal{W}_{40}\pm\sqrt{\frac{10}{7}}\mathcal{W}_{44}$
	2	1	3	1	$i\sqrt{\frac{3}{7}}\mathcal{W}_{10}-\frac{2i}{3}\mathcal{W}_{30}+\frac{5i}{3\sqrt{77}}\mathcal{W}_{50}\pm i\sqrt{\frac{10}{11}}\mathcal{W}_{54}$
	3	1	3	1	$\mathcal{W}_{00}-\frac{7}{11}\mathcal{W}_{40}+\frac{10}{11\sqrt{13}}\mathcal{W}_{60}\pm\frac{\sqrt{70}}{11}\mathcal{W}_{44}\pm\frac{10}{11}\sqrt{\frac{14}{13}}\mathcal{W}_{64}$
E	1	1	1	1	$\mathcal{W}_{00}-\frac{1}{\sqrt{5}}\mathcal{W}_{20}$
	1	1	2	1	$i\sqrt{\frac{3}{5}}\mathcal{W}_{10}-\frac{3i}{\sqrt{35}}\mathcal{W}_{30}$
	1	1	3	1	$-3\sqrt{\frac{2}{35}}\mathcal{W}_{20}+\sqrt{\frac{2}{7}}\mathcal{W}_{40}$
	1	1	3	2	$\frac{2}{\sqrt{3}}\mathcal{W}_{44}$
	2	1	2	1	$\mathcal{W}_{00}+\frac{\sqrt{5}}{7}\mathcal{W}_{20}-\frac{4}{7}\mathcal{W}_{40}$
	2	1	3	1	$2i\sqrt{\frac{6}{35}}\mathcal{W}_{10}+\frac{1}{3}i\sqrt{\frac{2}{5}}\mathcal{W}_{30}-\frac{5}{3}i\sqrt{\frac{10}{77}}\mathcal{W}_{50}$
	2	1	3	2	$-2i\sqrt{\frac{5}{33}}\mathcal{W}_{54}$
	3	1	3	1	$\mathcal{W}_{00}+\frac{1}{\sqrt{5}}\mathcal{W}_{20}+\frac{1}{11}\mathcal{W}_{40}-\frac{25}{11\sqrt{13}}\mathcal{W}_{60}$
	3	2	3	2	$\mathcal{W}_{00}-\frac{\sqrt{5}}{3}\mathcal{W}_{20}+\frac{3}{11}\mathcal{W}_{40}-\frac{5}{33\sqrt{13}}\mathcal{W}_{60}$

TABLE VIII. Non-zero reduced matrix elements for boosting in the cubic box (C_{4v} symmetry group) for integral angular momentum up to $J=3$. The A_2 sector does not appear below $J=4$. The B_1 and B_2 irreps are combined as indicated by the upper/lower signs. The matrix is hermitian in Jn and $J'n'$ in each irrep sector.

Γ	J	l		J'	l'		$\mathcal{M}^{\Gamma}_{Jl,J'l'}$
G_1	$\frac{1}{2}$	0		$\frac{1}{2}$	0		$\mathcal{W}_{00}$
	$\frac{1}{2}$	0		$\frac{1}{2}$	1		$-\frac{i}{\sqrt{3}}\mathcal{W}_{10}$
	$\frac{1}{2}$	0		$\frac{3}{2}$	1		$i\sqrt{\frac{2}{3}}\mathcal{W}_{10}$
	$\frac{1}{2}$	0		$\frac{3}{2}$	2		$\sqrt{\frac{2}{5}}\mathcal{W}_{20}$
	$\frac{1}{2}$	1		$\frac{3}{2}$	1		$-\sqrt{\frac{2}{5}}\mathcal{W}_{20}$
	$\frac{1}{2}$	1		$\frac{3}{2}$	2		$i\sqrt{\frac{2}{3}}\mathcal{W}_{10}$
	$\frac{3}{2}$	1		$\frac{3}{2}$	1		$\mathcal{W}_{00}+\frac{1}{\sqrt{5}}\mathcal{W}_{20}$
	$\frac{3}{2}$	1		$\frac{3}{2}$	2		$-i\frac{1}{5\sqrt{3}}\mathcal{W}_{10}-i\frac{9}{5\sqrt{7}}\mathcal{W}_{30}$
	$\frac{1}{2}$	0		$\frac{5}{2}$	2		$-\sqrt{\frac{3}{5}}\mathcal{W}_{20}$
	$\frac{1}{2}$	0		$\frac{5}{2}$	3		$i\sqrt{\frac{3}{7}}\mathcal{W}_{30}$
	$\frac{1}{2}$	1		$\frac{5}{2}$	3		$-i\sqrt{\frac{3}{7}}\mathcal{W}_{30}$
	$\frac{3}{2}$	1		$\frac{5}{2}$	2		$i\frac{3\sqrt{2}}{5}\mathcal{W}_{10}+\frac{2}{5}i\sqrt{\frac{6}{7}}\mathcal{W}_{30}$
	$\frac{3}{2}$	1		$\frac{5}{2}$	3		$\frac{1}{7}\sqrt{\frac{6}{5}}\mathcal{W}_{20}+\frac{2\sqrt{6}}{7}\mathcal{W}_{40}$
	$\frac{3}{2}$	2		$\frac{5}{2}$	2		$-\frac{1}{7}\sqrt{\frac{6}{5}}\mathcal{W}_{20}-\frac{2\sqrt{6}}{7}\mathcal{W}_{40}$
	$\frac{5}{2}$	2		$\frac{5}{2}$	2		$\mathcal{W}_{00}+\frac{8}{7\sqrt{5}}\mathcal{W}_{20}+\frac{2}{7}\mathcal{W}_{40}$
	$\frac{5}{2}$	2		$\frac{5}{2}$	3		$-i\frac{\sqrt{3}}{35}\mathcal{W}_{10}-i\frac{8}{15\sqrt{7}}\mathcal{W}_{30}-i\frac{50}{21\sqrt{11}}\mathcal{W}_{50}$
	J	l	n	J'	l'	n'	$\mathcal{M}^{\Gamma}_{Jln,J'l'n'}$
G_2	$\frac{3}{2}$	1	1	$\frac{3}{2}$	1	1	$\mathcal{W}_{00}-\frac{1}{\sqrt{5}}\mathcal{W}_{20}$
	$\frac{3}{2}$	1	1	$\frac{3}{2}$	2	1	$-i\frac{\sqrt{3}}{5}\mathcal{W}_{10}+i\frac{3}{5\sqrt{7}}\mathcal{W}_{30}$
	$\frac{3}{2}$	1	1	$\frac{5}{2}$	2	1	$i\frac{2\sqrt{3}}{5}\mathcal{W}_{10}-i\frac{6}{5\sqrt{7}}\mathcal{W}_{30}$
	$\frac{3}{2}$	1	1	$\frac{5}{2}$	3	1	$\frac{6}{7\sqrt{5}}\mathcal{W}_{20}-\frac{2}{7}\mathcal{W}_{40}$
	$\frac{3}{2}$	1	1	$\frac{5}{2}$	3	2	$-2\sqrt{\frac{2}{7}}\mathcal{W}_{44}$
	$\frac{3}{2}$	2	1	$\frac{5}{2}$	2	1	$-\frac{6}{7\sqrt{5}}\mathcal{W}_{20}+\frac{2}{7}\mathcal{W}_{40}$
	$\frac{3}{2}$	2	1	$\frac{5}{2}$	2	2	$2\sqrt{\frac{2}{7}}\mathcal{W}_{44}$
	$\frac{5}{2}$	2	1	$\frac{5}{2}$	2	1	$\mathcal{W}_{00}+\frac{2}{7\sqrt{5}}\mathcal{W}_{20}-\frac{3}{7}\mathcal{W}_{40}$
	$\frac{5}{2}$	2	1	$\frac{5}{2}$	2	2	$\sqrt{\frac{2}{7}}\mathcal{W}_{44}$
	$\frac{5}{2}$	2	2	$\frac{5}{2}$	2	2	$\mathcal{W}_{00}-\frac{2\sqrt{5}}{7}\mathcal{W}_{20}+\frac{1}{7}\mathcal{W}_{40}$
	$\frac{5}{2}$	2	1	$\frac{5}{2}$	3	1	$-i\frac{3\sqrt{3}}{35}\mathcal{W}_{10}-i\frac{2\sqrt{7}}{15}\mathcal{W}_{30}+i\frac{25}{21\sqrt{11}}\mathcal{W}_{50}$
	$\frac{5}{2}$	2	1	$\frac{5}{2}$	3	2	$5i\sqrt{\frac{2}{77}}\mathcal{W}_{54}$
	$\frac{5}{2}$	2	2	$\frac{5}{2}$	3	2	$i\frac{\sqrt{3}}{7}\mathcal{W}_{10}-i\frac{2}{3\sqrt{7}}\mathcal{W}_{30}+i\frac{5}{21\sqrt{11}}\mathcal{W}_{50}$

TABLE IX. Non-zero reduced matrix elements for boosting in the cubic box ($^2C_{4v}$ symmetry group) for half-integral angular momentum up to $J=5/2$. There is no multiplicity in the G_1 sector, but two-fold multiplicity in the G_2 sector. The horizontal lines separate different combinations of JJ'. The matrix is hermitian in Jln and $J'l'n'$ in each irrep sector.

In the G_2 sector, $\delta_{\frac{3}{2}1}$ and $\delta_{\frac{3}{2}2}$ become similarly coupled,

$$\begin{vmatrix} \mathcal{W}_{00} - \frac{1}{\sqrt{5}}\mathcal{W}_{20} - \cot\delta_{\frac{3}{2}1} & -i\frac{\sqrt{3}}{5}\mathcal{W}_{10} + i\frac{3}{5\sqrt{7}}\mathcal{W}_{30} \\ i\frac{\sqrt{3}}{5}\mathcal{W}_{10} - i\frac{3}{5\sqrt{7}}\mathcal{W}_{30} & \mathcal{W}_{00} - \frac{1}{\sqrt{5}}\mathcal{W}_{20} - \cot\delta_{\frac{3}{2}2} \end{vmatrix} = 0, \tag{69}$$

if we ignore mixing with higher J. So the determination of $\delta_{\frac{3}{2}1}$ (Δ or P_{33} resonance) requires four zeta functions ($\mathcal{W}_{l0}$ with $l = 0, 1, 2, 3$) and the knowledge of $\delta_{\frac{3}{2}2}$ (D_{33} resonance). Only when the $\delta_{\frac{3}{2}2}$ contribution can be ignored do we get the simple formula

$$\cot\delta_{\frac{3}{2}1} = \mathcal{W}_{00} - \frac{1}{\sqrt{5}}\mathcal{W}_{20}. \tag{70}$$

The above discussion applies to the general case of unequal masses. In the case of equal masses, parity is restored, and the tables simplify considerably. All the odd l zeta functions vanish and the matrix elements can be separated by irrep and parity. The same result can be reached by adding the boost directly to the results derived in the elongated box under the symmetry group ${}^2D_{4h}$, given in Table II and Table III. This perspective was adopted in Ref. [9], but it is only valid for equal masses.

Finally, we point out that in the limit when the boost goes to zero we recover the symmetry of the states at rest in elongated boxes. To see this just follow the subduction rules between ${}^2D_{4h}$ and ${}^2C_{4v}$ in Table VII. Indeed, Table VIII and Table IX go back to Table II and Table III after turning off the odd-l zeta functions, setting $\boldsymbol{d} = 0$ and $\gamma = 1$ in the remaining ones, and re-organizing by irrep and parity.

VIII. CONCLUSION

We have derived Lüscher phaseshift formulas for two-body elastic scattering in elongated boxes. We analyzed two scenarios: scattering of spinless mesons and scattering of a spin zero meson from a spin-1/2 baryon. For each of these scenarios we discussed the case where the two-body state is at rest with respect to the box, or moving along the elongated direction.

Our interest in elongated boxes stems from the fact that they allow us to vary the geometry of the box, and consequently the kinematics, with minimal amount of computer resources. On the other hand, elongated boxes have a different symmetry group than the cubic case and this has to be taken into account when designing interpolators and when connecting the infinite volume phase-shifts with the two-body energies.

The main goal of this study was to derive the relevant Lüscher formulas for π-N scattering on elongated boxes. To derive these relations we followed the methods developed for cubic boxes, while accounting for the different symmetry of our setup. The formulas derived for baryon-meson scattering in elongated boxes are, to our knowledge, new both for the moving and at-rest states. For the meson-meson scattering the formulas derived here for the states at rest agree with the one derived by in Ref. [6], while for the moving case they are mostly new. The only moving case considered in the literature was the A_2^- case for π-π scattering [9] and our results agree.

Elongated boxes offer a cost-effect way of varying the box size. The sensitivity of the energy spectrum to the elongation factor η is a channel-dependent problem. For an example in the $\pi\pi \to \rho$ channel, see our previous work in Ref. [9]. Generically, we expect these Lüscher phaseshift formulas to be valid up to corrections on the order of $e^{-m_\pi L}$.

As a validation of these formulas, we re-derived the results in the cubic box using the same approach that treats single and double-cover groups in a unified manner, as detailed in the appendices. How the symmetry is restored from the elongated box to the cubic box is governed by subduction rules and examples are given.

Boosting of the two-particle system in both the cubic and elongated boxes allows lower energies to be accessed, thus a wider coverage of the resonance region. The trade-off is the loss of parity for unequal masses which means mixing of even and odd states and generally more complicated formulas. We clarified the relationships between the various scenarios (cubic, elongated, and boosting) and how they transition from one another at the phaseshift level.

Finally, we note that the methods used here can be readily extended to other interesting cases. One example is the π-ρ scattering in the a_1 channel. Since ρ is not spinless, the formalism used here needs to be extended to a multi-channel one to account for the fact that the S-wave and D-wave states mix. However, if we consider that the S-wave channel dominates, some of the formulas derived here can be directly applied. Efforts are under way to investigate the a_1 and the Δ resonances using elongated boxes in lattice QCD simulations.

ACKNOWLEDGMENTS

This work is supported in part by the U.S. Department of Energy grant DE-FG02-95ER40907 and the National Science Foundation CAREER grant PHY-1151648. A.A. gratefully acknowledges the hospitality of the Physics Departments at the Universities of Maryland and Kentucky, and the Albert Einstein Center at the University of Bern where part of this work was carried out.

Appendix A: Symmetry group properties in the elongated box

In this appendix and the ones that follow, we give an overview of the basic ideas and terminology of group theory adapted for the understanding of angular momentum and phaseshift reduction in the elongated box. It is reasonably detailed for a coherent and self-contained picture. The literature on group theory is vast, coming from many perspectives including solid-state physics, quantum chemistry, and mathematics. We limit ourselves to a selected few [11–13, 15–17] that should be familiar to a student of physics.

In the elongated box (also known as a cuboid or square prism), the basic symmetry group involving only spatial rotations is called the dihedral group D_4. As far as group operations are concerned, the D_4 group is isomorphic to the symmetry of a square, with 8 simple elements (operations that return the square to itself). They can be divided into 5 conjugacy classes (operations that are equivalent): the identity (I), two $\pi/2$ rotations about the perpendicular z-axis ($2C_4$), one π rotation about the z-axis (C_2), two π rotations about x and y axes ($2C_2'$), and two π rotations about the two diagonals ($2C''_2$). The operations can be visualized in Fig. 1. To fully describe the physics at hand, we need two extensions. The box has a symmetry under space inversion (or parity) about the xy-plane, which entails the symmetry group D_{4h}. To describe half-integral angular momentum, the double-covered group of D_4, denoted as ${}^2D_4$, is required. So the full symmetry group in the elongated box will be called ${}^2D_{4h}$. All these variants will be explained below.

Given a group, a matrix representation can be constructed. The representations are generally not unique since a similarity transformation can lead to a different representation. What is unique is the *character* of each group element, defined as the trace of the matrix that represents the element. The character is the same within each conjugacy class. Usually representations of a finite group are reducible, so we seek the set of **irreducible representations** (hereafter referred to as **irreps**) for the group. One can think of the procedure as reducing a matrix in its block diagonal form by similarity transformations. For this reason, any representation of a finite group can be broken up into a direct sum of its irreps. Finding the irreps of a group is one of the most important tasks in group theory, followed by how things transform under the irreps.

The D_4 group has 5 irreps conventionally named A_1, A_2, B_1, B_2, and E, with respective dimensions 1, 1, 1, 1, 2 (whose squares sum to 8). It is an example of a general group property that the square of irrep dimensions sum to the total number of elements (or group order). Another useful property is that the number of irreps is equal to the number of conjugacy classes.

Table X summarizes all the ingredients for the elongated box. Some discussion is in order.

1. Single and double groups

In the continuum, the full rotation group is the $SO(3)$ group; its double-cover group is the $SU(2)$ group which is required for the inclusion of half-integer angular momentum. The concept of a double group can be understood by considering the character of the full rotation group given in Eq. 8. One can add an extra rotation of 2π to the character in that equation to yield the relation,

$$\chi(\omega + 2\pi, J) = (-1)^{2J}\chi(\omega, J). \tag{A1}$$

We see that the extra rotation leaves the character invariant for integer J as expected, but leads to a minus sign for half-integer J. So rotations by 4π are needed to leave the characters invariant (identity) for both integral and half-integral angular momentum. This property suggests a way to construct the double group from the single group: by adding a new group element $\mathcal{R}$ whose role is to perform an extra 2π rotation to all the elements in the single group. It will double the number of elements (hence the name double group, or double-covered group). The new element produced by the extra rotation on an single-group element C_k will be denoted by a tilde, $\mathcal{R}C_k = \widetilde{C_k}$. The number of conjugacy classes, on the other hand, will not simply double. The $\mathcal{R}C_3$ and $\mathcal{R}C_4$ will spawn new classes of elements not equivalent to C_3 or C_4 because adding 2π to $2\pi/3$ and $\pi/2$ leads to new rotations, but $\mathcal{R}C_2$ will belong in the same class as C_2 because adding 2π to π leads to the same rotations. When applied to the D_4 group elements, only two new classes emerge: $\widetilde{I}$ and $\widetilde{C}_4$. This means two new irreps in addition to the five existing ones. Their dimensions are constrained by $1^2 + 1^2 + 1^2 + 1^2 + 2^2 + l_6^2 + l_7^2 = 16$, or $l_6^2 + l_7^2 = 8$. The only solution is $l_6 = 2$, $l_7 = 2$. The two new two-dimensional irreps will be called G_1 and G_2. These two even-dimensional irreps are responsible for all half-integer angular momentum in the elongated box. Any irrep of the single group is also an irrep of the double group, with the same set of characters. For the new irreps, the characters for the class $\mathcal{R}C_k$ are the negative of the characters of class C_k, except for the $\mathcal{R}C_2$-type class for which the character is zero (when a real number is the negative of itself). These properties lead to most of the characters in the double group. Additionally, the character of the G_1 irrep in the C_3 class is simply that of a spinor $\chi(2\pi/3, 1/2) = 1$, and in the C_4 class $\chi(\pi/2, 1/2) = \sqrt{2}$. The rest of the entries can be readily worked out by the orthogonality conditions governing characters. The complete character

Class\Irrep	k	$\boldsymbol{n}$	ω	(α,β,γ)	A_1	A_2	B_1	B_2	E	G_1	G_2
I	1	$\{0,0,1\}$	4π	$\{0,0,0\}$	1	1	1	1	1	1	1
$\widetilde{I}$	2	$\{0,0,1\}$	2π	$\{0,0,2\pi\}$	1	1	1	1	1	-1	-1
C_{4z}^+	3	$\{0,0,1\}$	$\frac{\pi}{2}$	$\{0,0,\frac{\pi}{2}\}$	1	1	-1	-1	$-i\sigma_2$	$\frac{1-i\sigma_2}{\sqrt{2}}$	$\frac{-i\sigma_2-1}{\sqrt{2}}$
C_{4z}^-	4	$\{0,0,1\}$	$\frac{7\pi}{2}$	$\{0,0,\frac{7\pi}{2}\}$	1	1	-1	-1	$i\sigma_2$	$\frac{i\sigma_2+1}{\sqrt{2}}$	$\frac{i(\sigma_2+i)}{\sqrt{2}}$
$\widetilde{C}_{4z}^+$	5	$\{0,0,1\}$	$\frac{5\pi}{2}$	$\{0,0,\frac{5\pi}{2}\}$	1	1	-1	-1	$-i\sigma_2$	$\frac{i(\sigma_2+i)}{\sqrt{2}}$	$\frac{i\sigma_2+1}{\sqrt{2}}$
$\widetilde{C}_{4z}^-$	6	$\{0,0,1\}$	$\frac{3\pi}{2}$	$\{0,0,\frac{3\pi}{2}\}$	1	1	-1	-1	$i\sigma_2$	$\frac{-i\sigma_2-1}{\sqrt{2}}$	$\frac{1-i\sigma_2}{\sqrt{2}}$
C_{2z}	7	$\{0,0,1\}$	π	$\{0,0,\pi\}$	1	1	1	1	-1	$-i\sigma_2$	$i\sigma_2$
$\widetilde{C}_{2z}$	8	$\{0,0,1\}$	3π	$\{0,0,3\pi\}$	1	1	1	1	-1	$i\sigma_2$	$-i\sigma_2$
C_{2x}	9	$\{1,0,0\}$	π	$\{0,\pi,\pi\}$	1	-1	1	-1	σ_3	$i\sigma_3$	$i\sigma_3$
C_{2y}	10	$\{0,1,0\}$	π	$\{0,\pi,0\}$	1	-1	1	-1	$-\sigma_3$	$i\sigma_1$	$-i\sigma_1$
$\widetilde{C}_{2x}$	11	$\{1,0,0\}$	3π	$\{0,\pi,3\pi\}$	1	-1	1	-1	σ_3	$-i\sigma_3$	$-i\sigma_3$
$\widetilde{C}_{2y}$	12	$\{0,1,0\}$	3π	$\{0,\pi,2\pi\}$	1	-1	1	-1	$-\sigma_3$	$-i\sigma_1$	$i\sigma_1$
C_{2a}	13	$\{1,1,0\}$	π	$\{0,\pi,\frac{\pi}{2}\}$	1	-1	-1	1	σ_1	$\frac{i(\sigma_1+\sigma_3)}{\sqrt{2}}$	$\frac{i(\sigma_1-\sigma_3)}{\sqrt{2}}$
C_{2b}	14	$\{-1,1,0\}$	π	$\{0,\pi,\frac{7\pi}{2}\}$	1	-1	-1	1	$-\sigma_1$	$\frac{i(\sigma_1-\sigma_3)}{\sqrt{2}}$	$\frac{i(\sigma_1+\sigma_3)}{\sqrt{2}}$
$\widetilde{C}_{2a}$	15	$\{1,1,0\}$	3π	$\{0,\pi,\frac{5\pi}{2}\}$	1	-1	-1	1	σ_1	$-\frac{i(\sigma_1+\sigma_3)}{\sqrt{2}}$	$-\frac{i(\sigma_1-\sigma_3)}{\sqrt{2}}$
$\widetilde{C}_{2b}$	16	$\{-1,1,0\}$	3π	$\{0,\pi,\frac{3\pi}{2}\}$	1	-1	-1	1	$-\sigma_1$	$-\frac{i(\sigma_1-\sigma_3)}{\sqrt{2}}$	$-\frac{i(\sigma_1+\sigma_3)}{\sqrt{2}}$

TABLE X. Unified elements and irreps of the single D_4 group and double group ${}^2D_4$. The rotations are represented by the axis direction $\boldsymbol{n}$ (which should be normalized when in use) and rotation angle ω about the axis (which is defined over 4π). The horizontal lines separate the elements into 7 conjugacy classes. The two-dimensional representation matrices are expressed in terms of Pauli matrices.

${}^2D_4$	I	$\widetilde{I}$	$2C_4$	$2\widetilde{C}_4$	$C_2+\widetilde{C}_2$	$2C_2'+2\widetilde{C}_2'$	$2C_2''+2\widetilde{C}_2''$
A_1	1	1	1	1	1	1	1
A_2	1	1	1	1	1	-1	-1
B_1	1	1	-1	-1	1	1	-1
B_2	1	1	-1	-1	1	-1	1
E	2	2	0	0	-2	0	0
G_1	2	-2	$\sqrt{2}$	$-\sqrt{2}$	0	0	0
G_2	2	-2	$-\sqrt{2}$	$\sqrt{2}$	0	0	0
ω	4π	2π	$\pi/2$	$5\pi/2$	π	π	π

TABLE XI. Character table for the double group ${}^2D_4$. Last row is the angle of rotation about the axis in each class.

table is given in Table XI. It agrees with published tables (see for example Ref. [15]) (Note that the order of rows and columns in a character table does not matter). We also checked that the multiplication table (which is a necessary closure check of the group) from G_1 agrees with that in Ref. [15], and G_1 and G_2 have identical 16×16 multiplication tables. For most point groups, the character table can be constructed in the same manner, without knowing any representations of the group. Of course, one can readily extract the character table from the information given in Table X: for one-dimensional irreps the character is simply 1 or -1; for two-dimensional irreps the character is the trace of the representation matrix. The fact that the two methods agree provides a consistency check.

It should be emphasized that Table X is a unified presentation for both the single group D_4 and double group ${}^2D_4$. The above discussion makes clear the relationship between the two, and how to construct the double group from the single one. To obtain the table just for the single group, simply delete the tilded rows and the last two columns (G_1 and G_2).

The full symmetry group in the elongated box must include space inversion (parity). They are obtained by a direct product with the inversion group denoted by $C_i = \{I, i\}$ which has two elements, the identity and the inversion. Therefore, for the single group $D_{4h} = D_4 \otimes C_i$, and for the double group ${}^2D_{4h} = {}^2D_4 \otimes C_i$. In the case of D_{4h}, the group elements will double to 16, with 5 new inversion-related classes. The irreps will also double into two versions: 5 with even parity labeled by a plus sign (or g for *gerade*), 5 with odd parity labeled by a minus sign (or u for *ungerade*). The character table for D_{4h} can be constructed from that of D_4 by forming a super table 10×10 consisiting of 2×2 blocks of 5×5: adding a replica to the right and below, and its negative to the diagonal (see Ref. [15] for example). In similar fashion, the ${}^2D_{4h}$ group will double to 32 elements, 14 classes, and 7 even-parity and 7 odd-parity irreps. Its character table can be replicated from that of ${}^2D_4$ by forming a super table 14×14 consisting of 2×2 blocks of 7×7. In practice, however, we rarely have to work with the full content of D_{4h} or ${}^2D_{4h}$ groups. We can just work with D_4 or ${}^2D_4$, then include the consequence of space inversion fairly straightforwardly, *a posteriori*, as discussed in several places in the main text.

A useful physics consequence of this discussion is that angular momentum of both integer and half-integer values in the elongated box can be completely characterized by the 14 irreps of the ${}^2D_{4h}$ group. Section III A in the main text demonstrates how it is done.

2. Basis vectors in the elongated box

The irreps of the continuum rotation group with $J = 0, 1/2, 1, 3/2, \cdots$, are defined in the $(2J+1)$-dimensional space spanned on the basis vectors $|JM\rangle$, which are the standard spherical harmonics for integral J and the spin spherical harmonics for half-integral J. These representations are reducible under the ${}^2D_4$ group into its 7 irreps denoted by Γ. In other words, certain subspaces in the space spanned by $|JM\rangle$, are invariant under the symmetry transformations of the elongated box, furnishing irreps for the symmetry group. To find out basis vectors corresponding to a row α of irrep Γ we use the following projector:

$$P^\Gamma_\alpha = \sum_k (R^\Gamma_k)^*_{\alpha\alpha} O_k \tag{A2}$$

where k runs over the group elements, R^Γ_k is the matrix associated with rotation k in the Γ irrep and O_k is the operator that implements the rotation. For a $|JM\rangle$ states this operator is

$$O_k|JM\rangle = \sum_{M'=-J}^{J} D^J_{MM'}(\alpha_k, \beta_k, \gamma_k)|JM'\rangle \tag{A3}$$

where $D^J_{MM'}$ is the Wigner D-matrix as a function of Euler angles α, β, γ. In the case of one-dimensional irreps, R^Γ_k are simply the characters so the index α can be dropped. There is freedom to choose the overall phase factor and normalization factor. All the basis vectors are made orthonormal after they are found.

It should be pointed out that different matrix representations for the same irrep lead to different basis vectors. Since equivalent matrix representations are related by a similarity transformation, the set of basis vectors is related by the same similarity matrix. Physics results should be independent of this ambiguity. In the case of phaseshifts, the quantization condition involves determinants which are invariant under this transformation.

There is another feature in Table X that is worth pointing out. The rotations in the group elements are usually expressed as a rotation angle ω about a certain axis $\boldsymbol{n}$. In the case of spin 1/2,

$$D^{1/2}(\boldsymbol{n}, \omega) = \begin{pmatrix} \cos\frac{\omega}{2} - in_z \sin\frac{\omega}{2} & -(n_y + in_x)\sin\frac{\omega}{2} \\ (n_y - in_x)\sin\frac{\omega}{2} & \cos\frac{\omega}{2} + in_z \sin\frac{\omega}{2} \end{pmatrix}. \tag{A4}$$

But Euler angles are needed in the Wigner D-functions to construct the basis vectors,

$$D^{1/2}(\alpha, \beta, \gamma) = \begin{pmatrix} e^{-\frac{1}{2}i(\alpha+\gamma)}\cos\frac{\beta}{2} & -e^{-\frac{1}{2}i(\alpha-\gamma)}\sin\frac{\beta}{2} \\ e^{\frac{1}{2}i(\alpha-\gamma)}\sin\frac{\beta}{2} & e^{\frac{1}{2}i(\alpha+\gamma)}\cos\frac{\beta}{2} \end{pmatrix}. \tag{A5}$$

The traditionally-defined Euler angles are not unique (we use the standard active zyz notation in Ref. [13]). For example, when $\beta = 0$, only the combination $\alpha + \gamma$ is uniquely determined. Similarly, when $\beta = \pi$, only the combination $\alpha - \gamma$ is unique. Furthermore, double groups require rotations of $\omega = 4\pi$ to return identity for half-integral angular momentum. The Euler angles can be made unique by enlarging the domain of γ from 2π to 4π: $0 \le \alpha < 2\pi$, $0 \le \beta \le \pi$, $0 \le \gamma < 4\pi$, supplemented by the condition that $\alpha = 0$ when $\beta = 0$ or π (see [17]). In this way, there is an one-to-one correspondence between the two representations $D^{1/2}(\alpha,\beta,\gamma)$ and $D^{1/2}(\boldsymbol{n},\omega)$. The Euler angles thus determined are given in Table X. Another advantage of using the domain-extended Euler angles is in working with double groups. Traditionally, there is a sign ambiguity that has to be dealt with carefully, either by trial and error, or a factor system specially constructed to guarantee the one-to-one correspondence [15]. Because of the unique one-to-one correspondence using the domain-extended Euler angles, the signs for the tilded elements are automatically and correctly produced. For this reason, one can simply use a single-group table to represent double groups, thus saving a lot of space in presentation [17]. We choose to present the unified table of both single and double groups to make the relationship between the two explicit.

The basis vectors of ${}^2D_4$ are listed in Table XII. The entire set of basis vectors can be represented by the notation

$$|\Gamma\alpha Jln\rangle = \sum_M C^{\Gamma\alpha n}_{JlM}|JlM\rangle, \tag{A6}$$

where Γ stands for a given irrep of the group and α runs from 1 to the dimension of the irrep, n runs from 1 to $n(\Gamma,J)$, the multiplicity of J in irrep Γ. The coefficients $C^{\Gamma\alpha n}_{JlM}$ can be read off directly from the table. These coefficients are used in Section III B to reduce the matrix elements for phaseshifts.

Appendix B: Symmetry group properties in the cubic box

The discussion parallels the one for the elongated box in the previous appendix. We only outline the essential ingredients needed in the main text.

The symmetry group of the cube box consisting of only rotations is the octahedral (or cubic) point group, denoted by O. The O group can be visualized in Fig. 2. The 24 operations can be divided into 5 conjugacy classes: the identity (I); six $\pi/2$ rotations about the 3 axes ($6C_4$); three π rotations about the 3 axes ($3C_2$); eight $2\pi/3$ rotations about 4 body diagonals ($8C_3$); and six π rotations about axes parallel to 6 face diagonals ($6C_2'$). The O group has 5 unique irreps conventionally named A_1, A_2, E, T_1, and T_2, having respective dimensionality of 1, 1, 2, 3, 3 (whose squares sum to 24). To construct its double-covered group ${}^2O$, we add an extra 2π rotation to each of the 24 elements, which double its elements to 48. As a result, 3 new classes emerge: $\widetilde{I}$, $\widetilde{C}_3$ and $\widetilde{C}_4$. This means 3 new irreps in addition to the 5 existing ones. Their dimensions are constrained by $1^2+1^2+2^2+3^2+3^2+l_6^2+l_7^2+l_8^2=48$, or $l_6^2+l_7^2+l_8^2=24$. The only solution is the combination of 3 integers (2,2,4), which can be assigned as $l_6=2$, $l_7=2$, and $l_8=4$. The corresponding new irreps are called G_1, G_2, and H. These three even-dimensional irreps are responsible for all half-integer angular momentum in the cubic box. The complete character table for the ${}^2O$ is given in Table XIV. The full symmetry in the cubic box must also include space inversion. The corresponding group is called ${}^2O_h$ which can be constructed by a direct product of ${}^2O$ with the inversion group $C_i=\{I,i\}$. The ${}^2O_h$ has 96 elements and 16 irreps (8 even and 8 odd). The decomposition of angular momentum of both integer and half-integer values into the 16 irreps of the double group ${}^2O_h$ of the cubic box is given in Table IV.

A few words on the matrix representations in Table XIII. Operationally, A_1 is the identity representation. The T_1 rotates the geometrical vector (x,y,z) whose matrices t_k are generated via $e^{-i(\boldsymbol{n}\cdot\boldsymbol{J})\omega}$ where $(J_k)_{ij}=i\epsilon_{ijk}$, by running through the 48 elements in the order given (only distinct matrices are named). Similarly, the G_1 rotates the spinor whose matrices g_k are generated by $e^{-i(\boldsymbol{n}\cdot\boldsymbol{\sigma})\omega/2}$. The matrices for the four-dimensional H irrep h_k are generated by $e^{-i(\boldsymbol{n}\cdot\boldsymbol{J})\omega}$ where $\boldsymbol{J}$ are the generators of spin-3/2,

$$J_x=\begin{pmatrix}0&\frac{\sqrt3}{2}&0&0\\ \frac{\sqrt3}{2}&0&1&0\\ 0&1&0&\frac{\sqrt3}{2}\\ 0&0&\frac{\sqrt3}{2}&0\end{pmatrix},\ J_y=\begin{pmatrix}0&-\frac{i\sqrt3}{2}&0&0\\ \frac{i\sqrt3}{2}&0&-i&0\\ 0&i&0&-\frac{i\sqrt3}{2}\\ 0&0&\frac{i\sqrt3}{2}&0\end{pmatrix},\ J_z=\begin{pmatrix}\frac32&0&0&0\\ 0&\frac12&0&0\\ 0&0&-\frac12&0\\ 0&0&0&-\frac32\end{pmatrix}. \tag{B1}$$

For the remaining irreps, a sign change in the character of class $6C_4$ and $6C_2'$ connects A_2 to A_1, T_2 to T_1, and G_2 to G_1, respectively. The E is a real-valued, two-dimensional irrep whose matrices can be obtained from the fact that it has Cartesian basis vectors $\sqrt3(x^2-y^2)$ and $2z^2-x^2-y^2$ [15]. In other words, the T_1 rotations, which transform (x,y,z) to (x',y',z'), will transform the basis vectors according to

$$\begin{pmatrix}\sqrt3(x'^2-y'^2)\\ 2z'^2-x'^2-y'^2\end{pmatrix}=\begin{pmatrix}a_{11}&a_{12}\\ a_{21}&a_{22}\end{pmatrix}\begin{pmatrix}\sqrt3(x^2-y^2)\\ 2z^2-x^2-y^2\end{pmatrix}, \tag{B2}$$

where the coefficients form the matrix representation for the E irrep. The five distinct matrices thus obtained in

Γ	J	Basis in terms of $\vert JM\rangle$
A_1	0	$\vert 0,0\rangle$
	2	$\vert 2,0\rangle$
	4	$\vert 4,0\rangle$; $\frac{1}{\sqrt{2}}(\vert 4,4\rangle+\vert 4,-4\rangle)$
A_2	1	$\vert 1,0\rangle$
	3	$\vert 3,0\rangle$
	4	$\frac{1}{\sqrt{2}}(\vert 4,4\rangle-\vert 4,-4\rangle)$
B_1	2	$\frac{1}{\sqrt{2}}(\vert 2,2\rangle+\vert 2,-2\rangle)$
	3	$\frac{1}{\sqrt{2}}(\vert 3,2\rangle-\vert 3,-2\rangle)$
	4	$\frac{1}{\sqrt{2}}(\vert 4,2\rangle+\vert 4,-2\rangle)$
B_2	2	$\frac{1}{\sqrt{2}}(\vert 2,2\rangle-\vert 2,-2\rangle)$
	3	$\frac{1}{\sqrt{2}}(\vert 3,2\rangle+\vert 3,-2\rangle)$
	4	$\frac{1}{\sqrt{2}}(\vert 4,2\rangle-\vert 4,-2\rangle)$
E	1	$\frac{1}{\sqrt{2}}(\vert 1,1\rangle\mp\vert 1,-1\rangle)$
	2	$\frac{1}{\sqrt{2}}(\vert 2,1\rangle\pm\vert 2,-1\rangle)$
	3	$\frac{1}{\sqrt{2}}(\vert 3,1\rangle\mp\vert 3,-1\rangle)$; $\frac{1}{\sqrt{2}}(\mp\vert 3,3\rangle+\vert 3,-3\rangle)$
	4	$\frac{1}{\sqrt{2}}(\vert 4,1\rangle\pm\vert 4,-1\rangle)$; $\frac{1}{\sqrt{2}}(\pm\vert 4,3\rangle+\vert 4,-3\rangle)$
G_1	$\frac{1}{2}$	$\frac{1}{\sqrt{2}}\left(\left\vert\frac{1}{2},\frac{1}{2}\right\rangle\mp\left\vert\frac{1}{2},-\frac{1}{2}\right\rangle\right)$
	$\frac{3}{2}$	$\frac{1}{\sqrt{2}}\left(\left\vert\frac{3}{2},\frac{1}{2}\right\rangle\pm\left\vert\frac{3}{2},-\frac{1}{2}\right\rangle\right)$
	$\frac{5}{2}$	$\frac{1}{\sqrt{2}}\left(\left\vert\frac{5}{2},\frac{1}{2}\right\rangle\mp\left\vert\frac{5}{2},-\frac{1}{2}\right\rangle\right)$
	$\frac{7}{2}$	$\frac{1}{\sqrt{2}}\left(\left\vert\frac{7}{2},\frac{1}{2}\right\rangle\pm\left\vert\frac{7}{2},-\frac{1}{2}\right\rangle\right)$; $\frac{1}{\sqrt{2}}\left(\pm\left\vert\frac{7}{2},\frac{7}{2}\right\rangle+\left\vert\frac{7}{2},-\frac{7}{2}\right\rangle\right)$
G_2	$\frac{3}{2}$	$\frac{1}{\sqrt{2}}\left(\left\vert\frac{3}{2},\frac{3}{2}\right\rangle\pm\left\vert\frac{3}{2},-\frac{3}{2}\right\rangle\right)$
	$\frac{5}{2}$	$\frac{1}{\sqrt{2}}\left(\left\vert\frac{5}{2},\frac{3}{2}\right\rangle\mp\left\vert\frac{5}{2},-\frac{3}{2}\right\rangle\right)$; $\frac{1}{\sqrt{2}}\left(\mp\left\vert\frac{5}{2},\frac{5}{2}\right\rangle+\left\vert\frac{5}{2},-\frac{5}{2}\right\rangle\right)$
	$\frac{7}{2}$	$\frac{1}{\sqrt{2}}\left(\left\vert\frac{7}{2},\frac{3}{2}\right\rangle\pm\left\vert\frac{7}{2},-\frac{3}{2}\right\rangle\right)$; $\frac{1}{\sqrt{2}}\left(\pm\left\vert\frac{7}{2},\frac{5}{2}\right\rangle+\left\vert\frac{7}{2},-\frac{5}{2}\right\rangle\right)$

TABLE XII. Basis vectors for the double dihedral group ${}^2D_4$ for total angular momentum up to $J=4$. The two-dimensional irreps (E, G_1, G_2) have two components indicated by upper/lower signs. Some irreps have two vectors for certain J values (multiplicities) indicated by semicolons.

Table XIII are

$$e_1=\begin{pmatrix}-1 & 0\\ 0 & 1\end{pmatrix}\quad e_2=\begin{pmatrix}-\frac{1}{2} & -\frac{\sqrt{3}}{2}\\ \frac{\sqrt{3}}{2} & -\frac{1}{2}\end{pmatrix}\quad e_3=\begin{pmatrix}-\frac{1}{2} & \frac{\sqrt{3}}{2}\\ -\frac{\sqrt{3}}{2} & -\frac{1}{2}\end{pmatrix}\quad e_4=\begin{pmatrix}\frac{1}{2} & -\frac{\sqrt{3}}{2}\\ -\frac{\sqrt{3}}{2} & -\frac{1}{2}\end{pmatrix}\quad e_5=\begin{pmatrix}\frac{1}{2} & \frac{\sqrt{3}}{2}\\ \frac{\sqrt{3}}{2} & -\frac{1}{2}\end{pmatrix}. \tag{B3}$$

We also checked that G_1, G_2, and H have identical 48×48 multiplication tables.

It is worth emphasizing that the representation matrices for the multi-dimensional irreps generated by running through the 48 elements in the given order automatically acquire the correct signs for both single and double groups. The rotation axis $\boldsymbol{n}$ and the angle ω have one-to-one correspondence to the domain-extended Euler angles, as discussed in the previous appendix. The basis vectors from the Euler angles in the cubic box are given in Table XV.

k	Elem	$\boldsymbol{n}$	ω	$\{\alpha,\beta,\gamma\}$	A_1	A_2	E	T_1	T_2	G_1	G_2	H
1	I	$\{0,0,1\}$	4π	$\{0,0,0\}$	1	1	$\mathbb{1}$	t_1	t_1	g_1	g_1	h_1
2	$\widetilde{I}$	$\{0,0,1\}$	2π	$\{0,0,2\pi\}$	1	1	$\mathbb{1}$	t_1	t_1	$-g_1$	$-g_1$	$-h_1$
3	C_{2x}	$\{1,0,0\}$	π	$\{0,\pi,\pi\}$	1	1	$\mathbb{1}$	t_2	t_2	g_2	g_2	h_2
4	C_{2y}	$\{0,1,0\}$	π	$\{0,\pi,0\}$	1	1	$\mathbb{1}$	t_3	t_3	g_3	g_3	h_3
5	C_{2z}	$\{0,0,1\}$	π	$\{0,0,\pi\}$	1	1	$\mathbb{1}$	t_4	t_4	g_4	g_4	h_4
6	$\widetilde{C}_{2x}$	$\{1,0,0\}$	3π	$\{0,\pi,3\pi\}$	1	1	$\mathbb{1}$	t_2	t_2	$-g_2$	$-g_2$	$-h_2$
7	$\widetilde{C}_{2y}$	$\{0,1,0\}$	3π	$\{0,\pi,2\pi\}$	1	1	$\mathbb{1}$	t_3	t_3	$-g_3$	$-g_3$	$-h_3$
8	$\widetilde{C}_{2z}$	$\{0,0,1\}$	3π	$\{0,0,3\pi\}$	1	1	$\mathbb{1}$	t_4	t_4	$-g_4$	$-g_4$	$-h_4$
9	C_{31}^+	$\{1,1,1\}$	$\frac{2\pi}{3}$	$\{0,\frac{\pi}{2},\frac{\pi}{2}\}$	1	1	e_3	t_5	t_5	g_5	g_5	h_5
10	C_{32}^+	$\{-1,-1,1\}$	$\frac{2\pi}{3}$	$\{\pi,\frac{\pi}{2},\frac{7\pi}{2}\}$	1	1	e_3	t_6	t_6	g_6	g_6	h_6
11	C_{33}^+	$\{1,-1,-1\}$	$\frac{2\pi}{3}$	$\{\pi,\frac{\pi}{2},\frac{5\pi}{2}\}$	1	1	e_3	t_7	t_7	g_7	g_7	h_7
12	C_{34}^+	$\{-1,1,-1\}$	$\frac{2\pi}{3}$	$\{0,\frac{\pi}{2},\frac{7\pi}{2}\}$	1	1	e_3	t_8	t_8	g_8	g_8	h_8
13	C_{31}^-	$\{1,1,1\}$	$\frac{10\pi}{3}$	$\{\frac{\pi}{2},\frac{\pi}{2},3\pi\}$	1	1	e_2	t_9	t_9	g_9	g_9	h_9
14	C_{32}^-	$\{-1,-1,1\}$	$\frac{10\pi}{3}$	$\{\frac{3\pi}{2},\frac{\pi}{2},2\pi\}$	1	1	e_2	t_{10}	t_{10}	g_{10}	g_{10}	h_{10}
15	C_{33}^-	$\{1,-1,-1\}$	$\frac{10\pi}{3}$	$\{\frac{\pi}{2},\frac{\pi}{2},0\}$	1	1	e_2	t_{11}	t_{11}	g_{11}	g_{11}	h_{11}
16	C_{34}^-	$\{-1,1,-1\}$	$\frac{10\pi}{3}$	$\{\frac{3\pi}{2},\frac{\pi}{2},3\pi\}$	1	1	e_2	t_{12}	t_{12}	g_{12}	g_{12}	h_{12}
17	$\widetilde{C}_{31}^+$	$\{1,1,1\}$	$\frac{8\pi}{3}$	$\{0,\frac{\pi}{2},\frac{5\pi}{2}\}$	1	1	e_3	t_5	t_5	$-g_5$	$-g_5$	$-h_5$
18	$\widetilde{C}_{32}^+$	$\{-1,-1,1\}$	$\frac{8\pi}{3}$	$\{\pi,\frac{\pi}{2},\frac{3\pi}{2}\}$	1	1	e_3	t_6	t_6	$-g_6$	$-g_6$	$-h_6$
19	$\widetilde{C}_{33}^+$	$\{1,-1,-1\}$	$\frac{8\pi}{3}$	$\{\pi,\frac{\pi}{2},\frac{\pi}{2}\}$	1	1	e_3	t_7	t_7	$-g_7$	$-g_7$	$-h_7$
20	$\widetilde{C}_{34}^+$	$\{-1,1,-1\}$	$\frac{8\pi}{3}$	$\{0,\frac{\pi}{2},\frac{3\pi}{2}\}$	1	1	e_3	t_8	t_8	$-g_8$	$-g_8$	$-h_8$
21	$\widetilde{C}_{31}^-$	$\{1,1,1\}$	$\frac{4\pi}{3}$	$\{\frac{\pi}{2},\frac{\pi}{2},\pi\}$	1	1	e_2	t_9	t_9	$-g_9$	$-g_9$	$-h_9$
22	$\widetilde{C}_{32}^-$	$\{-1,-1,1\}$	$\frac{4\pi}{3}$	$\{\frac{3\pi}{2},\frac{\pi}{2},0\}$	1	1	e_2	t_{10}	t_{10}	$-g_{10}$	$-g_{10}$	$-h_{10}$
23	$\widetilde{C}_{33}^-$	$\{1,-1,-1\}$	$\frac{4\pi}{3}$	$\{\frac{\pi}{2},\frac{\pi}{2},2\pi\}$	1	1	e_2	t_{11}	t_{11}	$-g_{11}$	$-g_{11}$	$-h_{11}$
24	$\widetilde{C}_{34}^-$	$\{-1,1,-1\}$	$\frac{4\pi}{3}$	$\{\frac{3\pi}{2},\frac{\pi}{2},\pi\}$	1	1	e_2	t_{12}	t_{12}	$-g_{12}$	$-g_{12}$	$-h_{12}$
25	C_{4x}^+	$\{1,0,0\}$	$\frac{\pi}{2}$	$\{\frac{3\pi}{2},\frac{\pi}{2},\frac{5\pi}{2}\}$	1	-1	e_4	t_{13}	$-t_{13}$	g_{13}	$-g_{13}$	h_{13}
26	C_{4y}^+	$\{0,1,0\}$	$\frac{\pi}{2}$	$\{0,\frac{\pi}{2},0\}$	1	-1	e_5	t_{14}	$-t_{14}$	g_{14}	$-g_{14}$	h_{14}
27	C_{4z}^+	$\{0,0,1\}$	$\frac{\pi}{2}$	$\{0,0,\frac{\pi}{2}\}$	1	-1	e_1	t_{15}	$-t_{15}$	g_{15}	$-g_{15}$	h_{15}
28	C_{4x}^-	$\{1,0,0\}$	$\frac{7\pi}{2}$	$\{\frac{\pi}{2},\frac{\pi}{2},\frac{7\pi}{2}\}$	1	-1	e_4	t_{16}	$-t_{16}$	g_{16}	$-g_{16}$	h_{16}
29	C_{4y}^-	$\{0,1,0\}$	$\frac{7\pi}{2}$	$\{\pi,\frac{\pi}{2},3\pi\}$	1	-1	e_5	t_{17}	$-t_{17}$	g_{17}	$-g_{17}$	h_{17}
30	C_{4z}^-	$\{0,0,1\}$	$\frac{7\pi}{2}$	$\{0,0,\frac{7\pi}{2}\}$	1	-1	e_1	t_{18}	$-t_{18}$	g_{18}	$-g_{18}$	h_{18}
31	$\widetilde{C}_{4x}^+$	$\{1,0,0\}$	$\frac{5\pi}{2}$	$\{\frac{3\pi}{2},\frac{\pi}{2},\frac{\pi}{2}\}$	1	-1	e_4	t_{13}	$-t_{13}$	$-g_{13}$	g_{13}	$-h_{13}$
32	$\widetilde{C}_{4y}^+$	$\{0,1,0\}$	$\frac{5\pi}{2}$	$\{0,\frac{\pi}{2},2\pi\}$	1	-1	e_5	t_{14}	$-t_{14}$	$-g_{14}$	g_{14}	$-h_{14}$
33	$\widetilde{C}_{4z}^+$	$\{0,0,1\}$	$\frac{5\pi}{2}$	$\{0,0,\frac{5\pi}{2}\}$	1	-1	e_1	t_{15}	$-t_{15}$	$-g_{15}$	g_{15}	$-h_{15}$
34	$\widetilde{C}_{4x}^-$	$\{1,0,0\}$	$\frac{3\pi}{2}$	$\{\frac{\pi}{2},\frac{\pi}{2},\frac{3\pi}{2}\}$	1	-1	e_4	t_{16}	$-t_{16}$	$-g_{16}$	g_{16}	$-h_{16}$
35	$\widetilde{C}_{4y}^-$	$\{0,1,0\}$	$\frac{3\pi}{2}$	$\{\pi,\frac{\pi}{2},\pi\}$	1	-1	e_5	t_{17}	$-t_{17}$	$-g_{17}$	g_{17}	$-h_{17}$
36	$\widetilde{C}_{4z}^-$	$\{0,0,1\}$	$\frac{3\pi}{2}$	$\{0,0,\frac{3\pi}{2}\}$	1	-1	e_1	t_{18}	$-t_{18}$	$-g_{18}$	g_{18}	$-h_{18}$
37	C_{2a}	$\{1,1,0\}$	π	$\{0,\pi,\frac{\pi}{2}\}$	1	-1	e_1	t_{19}	$-t_{19}$	g_{19}	$-g_{19}$	h_{19}
38	C_{2b}	$\{-1,1,0\}$	π	$\{0,\pi,\frac{7\pi}{2}\}$	1	-1	e_1	t_{20}	$-t_{20}$	g_{20}	$-g_{20}$	h_{20}
39	C_{2c}	$\{1,0,1\}$	π	$\{0,\frac{\pi}{2},\pi\}$	1	-1	e_5	t_{21}	$-t_{21}$	g_{21}	$-g_{21}$	h_{21}
40	C_{2d}	$\{0,1,1\}$	π	$\{\frac{\pi}{2},\frac{\pi}{2},\frac{\pi}{2}\}$	1	-1	e_4	t_{22}	$-t_{22}$	g_{22}	$-g_{22}$	h_{22}
41	C_{2e}	$\{-1,0,1\}$	π	$\{\pi,\frac{\pi}{2},0\}$	1	-1	e_5	t_{23}	$-t_{23}$	g_{23}	$-g_{23}$	h_{23}
42	C_{2f}	$\{0,-1,1\}$	π	$\{\frac{3\pi}{2},\frac{\pi}{2},\frac{7\pi}{2}\}$	1	-1	e_4	t_{24}	$-t_{24}$	g_{24}	$-g_{24}$	h_{24}
43	$\widetilde{C}_{2a}$	$\{1,1,0\}$	3π	$\{0,\pi,\frac{5\pi}{2}\}$	1	-1	e_1	t_{19}	$-t_{19}$	$-g_{19}$	g_{19}	$-h_{19}$
44	$\widetilde{C}_{2b}$	$\{-1,1,0\}$	3π	$\{0,\pi,\frac{3\pi}{2}\}$	1	-1	e_1	t_{20}	$-t_{20}$	$-g_{20}$	g_{20}	$-h_{20}$
45	$\widetilde{C}_{2c}$	$\{1,0,1\}$	3π	$\{0,\frac{\pi}{2},3\pi\}$	1	-1	e_5	t_{21}	$-t_{21}$	$-g_{21}$	g_{21}	$-h_{21}$
46	$\widetilde{C}_{2d}$	$\{0,1,1\}$	3π	$\{\frac{\pi}{2},\frac{\pi}{2},\frac{5\pi}{2}\}$	1	-1	e_4	t_{22}	$-t_{22}$	$-g_{22}$	g_{22}	$-h_{22}$
47	$\widetilde{C}_{2e}$	$\{-1,0,1\}$	3π	$\{\pi,\frac{\pi}{2},2\pi\}$	1	-1	e_5	t_{23}	$-t_{23}$	$-g_{23}$	g_{23}	$-h_{23}$
48	$\widetilde{C}_{2f}$	$\{0,-1,1\}$	3π	$\{\frac{3\pi}{2},\frac{\pi}{2},\frac{3\pi}{2}\}$	1	-1	e_4	t_{24}	$-t_{24}$	$-g_{24}$	g_{24}	$-h_{24}$

TABLE XIII. Unified elements and irreps of the single cubic group O and double cubic group ${}^2O$. The rotations are represented by the axis direction $\boldsymbol{n}$ (which should be normalized) and rotation angle ω about the axis (which is defined over 4π). The horizontal lines separate the elements into 8 conjugacy classes.

^2O	I	$\widetilde{I}$	$3C_2+3\widetilde{C}_2$	$8C_3$	$8\widetilde{C}_3$	$6C_4$	$6\widetilde{C}_4$	$6C_2'+6\widetilde{C}_2'$
A_1	1	1	1	1	1	1	1	1
A_2	1	1	1	1	1	-1	-1	-1
E	2	2	2	-1	-1	0	0	0
T_1	3	3	-1	0	0	1	1	-1
T_2	3	3	-1	0	0	-1	-1	1
G_1	2	-2	0	1	-1	$\sqrt{2}$	$-\sqrt{2}$	0
G_2	2	-2	0	1	-1	$-\sqrt{2}$	$\sqrt{2}$	0
H	4	-4	0	-1	1	0	0	0
ω	4π	2π	π	$2\pi/3$	$4\pi/3$	$\pi/2$	$3\pi/2$	π

TABLE XIV. Character table for the double octahedral group ^2O. Last row is the angle of rotation about the axis in each class.

Γ	J	l	Basis in terms of $\|JM\rangle$
A_1	0		$\|0,0\rangle$
	4		$\frac{\sqrt{21}}{6}\|4,0\rangle+\frac{\sqrt{30}}{12}(\|4,4\rangle+\|4,-4\rangle)$
A_2	3		$\frac{1}{\sqrt{2}}(\|3,2\rangle-\|3,-2\rangle)$
E	2		$\|2,0\rangle;\ \frac{1}{\sqrt{2}}(\|2,2\rangle+\|2,-2\rangle)$
	4		$\frac{1}{\sqrt{2}}(\|4,2\rangle+\|4,-2\rangle);\ \frac{\sqrt{15}}{6}\|4,0\rangle-\frac{\sqrt{42}}{12}(\|4,4\rangle+\|4,-4\rangle)$
T_1	1		$\|1,0\rangle;\ \frac{1}{\sqrt{2}}(\|1,1\rangle-\|1,-1\rangle);\ \frac{i}{\sqrt{2}}(\|1,1\rangle+\|1,-1\rangle)$
	3		$\|3,0\rangle;\ \frac{\sqrt{3}}{4}(\|3,1\rangle-\|3,-1\rangle)-\frac{\sqrt{5}}{4}(\|3,3\rangle-\|3,-3\rangle);\ -\frac{i\sqrt{3}}{4}(\|3,1\rangle+\|3,-1\rangle)-\frac{i\sqrt{5}}{4}(\|3,3\rangle+\|3,-3\rangle)$
	4		$-\frac{1}{\sqrt{2}}(\|4,4\rangle-\|4,-4\rangle);\ -\frac{1}{4}(\|4,3\rangle+\|4,-3\rangle)-\frac{\sqrt{7}}{4}(\|4,1\rangle+\|4,-1\rangle);\ -\frac{i}{4}(\|4,3\rangle-\|4,-3\rangle)+\frac{i\sqrt{7}}{4}(\|4,1\rangle-\|4,-1\rangle)$
T_2	1		$-\frac{1}{\sqrt{2}}(\|2,1\rangle+\|2,-1\rangle);\ -\frac{i}{\sqrt{2}}(\|2,1\rangle-\|2,-1\rangle);\ \frac{1}{\sqrt{2}}(\|2,2\rangle-\|2,-2\rangle)$
	3		$\frac{1}{\sqrt{2}}(\|3,2\rangle+\|3,-2\rangle);\ \frac{\sqrt{5}}{4}(\|3,1\rangle-\|3,-1\rangle)+\frac{\sqrt{3}}{4}(\|3,3\rangle-\|3,-3\rangle);\ \frac{i\sqrt{5}}{4}(\|3,1\rangle+\|3,-1\rangle)-\frac{i\sqrt{3}}{4}(\|3,3\rangle+\|3,-3\rangle)$
	4		$-\frac{1}{\sqrt{2}}(\|4,2\rangle-\|4,-2\rangle);\ -\frac{1}{4}(\|4,1\rangle+\|4,-1\rangle)+\frac{\sqrt{7}}{4}(\|4,3\rangle+\|4,-3\rangle);\ -\frac{i}{4}(\|4,1\rangle-\|4,-1\rangle)-\frac{i\sqrt{7}}{4}(\|4,3\rangle-\|4,-3\rangle)$
G_1	$\frac{1}{2}$	0, 1	$\|\frac{1}{2},\frac{1}{2}\rangle;\ \|\frac{1}{2},-\frac{1}{2}\rangle$
	$\frac{7}{2}$	3, 4	$-\frac{\sqrt{15}}{6}\|\frac{7}{2},\frac{7}{2}\rangle-\frac{\sqrt{21}}{6}\|\frac{7}{2},-\frac{1}{2}\rangle;\ \frac{\sqrt{15}}{6}\|\frac{7}{2},-\frac{7}{2}\rangle+\frac{\sqrt{21}}{6}\|\frac{7}{2},\frac{1}{2}\rangle$
G_2	$\frac{5}{2}$	2, 3	$-\frac{\sqrt{6}}{6}\|\frac{5}{2},\frac{5}{2}\rangle+\frac{\sqrt{30}}{6}\|\frac{5}{2},-\frac{3}{2}\rangle;\ -\frac{\sqrt{6}}{6}\|\frac{5}{2},-\frac{5}{2}\rangle+\frac{\sqrt{30}}{6}\|\frac{5}{2},\frac{3}{2}\rangle$
	$\frac{7}{2}$	3, 4	$\frac{\sqrt{3}}{2}\|\frac{7}{2},\frac{5}{2}\rangle-\frac{1}{2}\|\frac{7}{2},-\frac{3}{2}\rangle;\ -\frac{\sqrt{3}}{2}\|\frac{7}{2},-\frac{5}{2}\rangle+\frac{1}{2}\|\frac{7}{2},\frac{3}{2}\rangle$
H	$\frac{3}{2}$	1, 2	$\|\frac{3}{2},\frac{3}{2}\rangle;\ \|\frac{3}{2},-\frac{3}{2}\rangle;\ \|\frac{3}{2},\frac{1}{2}\rangle;\ \|\frac{3}{2},-\frac{1}{2}\rangle$
	$\frac{5}{2}$	2, 3	$\|\frac{5}{2},\frac{1}{2}\rangle;\ -\|\frac{5}{2},-\frac{1}{2}\rangle;\ \frac{\sqrt{30}}{6}\|\frac{5}{2},\frac{5}{2}\rangle+\frac{\sqrt{6}}{6}\|\frac{5}{2},-\frac{3}{2}\rangle;\ -\frac{\sqrt{30}}{6}\|\frac{5}{2},-\frac{5}{2}\rangle-\frac{\sqrt{6}}{6}\|\frac{5}{2},\frac{3}{2}\rangle$
	$\frac{7}{2}$	3, 4	$\frac{\sqrt{21}}{6}\|\frac{7}{2},\frac{7}{2}\rangle-\frac{\sqrt{15}}{6}\|\frac{7}{2},-\frac{1}{2}\rangle;\ \frac{\sqrt{21}}{6}\|\frac{7}{2},-\frac{7}{2}\rangle-\frac{\sqrt{15}}{6}\|\frac{7}{2},\frac{1}{2}\rangle;\ \frac{1}{2}\|\frac{7}{2},\frac{5}{2}\rangle+\frac{\sqrt{3}}{2}\|\frac{7}{2},-\frac{3}{2}\rangle;\ \frac{1}{2}\|\frac{7}{2},-\frac{5}{2}\rangle+\frac{\sqrt{3}}{2}\|\frac{7}{2},\frac{3}{2}\rangle;$

TABLE XV. Basis vectors of the double cubic group ^2O for total angular momentum up to $J=4$. The components for multi-dimensional irreps are indicated by semicolons. There are no multiplicities up to this J cutoff.

Appendix C: Basis vectors for boosting ($^2C_{4v}$ group)

Boosting singles out a special direction so the group symmetry is reduced. For boosts in the z-direction, the symmetry is reduced from the O_h group to its subgroup C_{4v} (the little group), or from its double cover ^2O_h to $^2C_{4v}$ when half-integral angular momentum is involved. The C_{4v} group has eight elements, divided into five conjugacy classes: the identity (I), two $\pi/2$ rotations about the z-axis ($2C_4$), one π rotation about the z-axis (C_2), two mirror reflections about xz and yz planes ($2\sigma_v$), and two mirror reflections about the two diagonal planes containing the z-axis ($2\sigma_d$). One can identify these operations from those of the full cubic group (both single O_h and double ^2O_h)

Γ	J	Basis $\lvert JM\rangle$ (even branch)	Basis $\lvert JM\rangle$ (odd branch)
A_1	0	$\lvert 0,0\rangle$	
	1		$\lvert 1,0\rangle$
	2	$\lvert 2,0\rangle$	
	3		$\lvert 3,0\rangle$
	4	$\lvert 4,0\rangle$; $\frac{1}{\sqrt{2}}(\lvert 4,4\rangle + \lvert 4,-4\rangle)$	
A_2	4	$\frac{1}{\sqrt{2}}(\lvert 4,4\rangle - \lvert 4,-4\rangle)$	
B_1	2	$\frac{1}{\sqrt{2}}(\lvert 2,2\rangle + \lvert 2,-2\rangle)$	
	3		$\frac{1}{\sqrt{2}}(\lvert 3,2\rangle + \lvert 3,-2\rangle)$
	4	$\frac{1}{\sqrt{2}}(\lvert 4,2\rangle + \lvert 4,-2\rangle)$	
B_2	2	$\frac{1}{\sqrt{2}}(\lvert 2,2\rangle - \lvert 2,-2\rangle)$	
	3		$\frac{1}{\sqrt{2}}(\lvert 3,2\rangle - \lvert 3,-2\rangle)$
	4	$\frac{1}{\sqrt{2}}(\lvert 4,2\rangle - \lvert 4,-2\rangle)$	
E	1		$\frac{1}{\sqrt{2}}(\lvert 1,1\rangle \pm \lvert 1,-1\rangle)$
	2	$\frac{1}{\sqrt{2}}(\lvert 2,1\rangle \pm \lvert 2,-1\rangle)$	
	3		$\frac{1}{\sqrt{2}}(\lvert 3,1\rangle \pm \lvert 3,-1\rangle)$; $\frac{1}{\sqrt{2}}(\pm\lvert 3,3\rangle + \lvert 3,-3\rangle)$
	4	$\frac{1}{\sqrt{2}}(\lvert 4,1\rangle \pm \lvert 4,-1\rangle)$; $\frac{1}{\sqrt{2}}(\pm\lvert 4,3\rangle + \lvert 4,-3\rangle)$	
G_1	$\frac{1}{2}$	$\frac{1}{\sqrt{2}}\left(\lvert\frac{1}{2},\frac{1}{2}\rangle \mp \lvert\frac{1}{2},-\frac{1}{2}\rangle\right)$	$\frac{1}{\sqrt{2}}\left(\lvert\frac{1}{2},\frac{1}{2}\rangle \pm \lvert\frac{1}{2},-\frac{1}{2}\rangle\right)$
	$\frac{3}{2}$	$\frac{1}{\sqrt{2}}\left(\lvert\frac{3}{2},\frac{1}{2}\rangle \pm \lvert\frac{3}{2},-\frac{1}{2}\rangle\right)$	$\frac{1}{\sqrt{2}}\left(\lvert\frac{3}{2},\frac{1}{2}\rangle \mp \lvert\frac{3}{2},-\frac{1}{2}\rangle\right)$
	$\frac{5}{2}$	$\frac{1}{\sqrt{2}}\left(\lvert\frac{5}{2},\frac{1}{2}\rangle \mp \lvert\frac{5}{2},-\frac{1}{2}\rangle\right)$	$\frac{1}{\sqrt{2}}\left(\lvert\frac{5}{2},\frac{1}{2}\rangle \pm \lvert\frac{5}{2},-\frac{1}{2}\rangle\right)$
	$\frac{7}{2}$	$\frac{1}{\sqrt{2}}\left(\lvert\frac{7}{2},\frac{1}{2}\rangle \pm \lvert\frac{7}{2},-\frac{1}{2}\rangle\right)$; $\frac{1}{\sqrt{2}}\left(\pm\lvert\frac{7}{2},\frac{7}{2}\rangle + \lvert\frac{7}{2},-\frac{7}{2}\rangle\right)$	$\frac{1}{\sqrt{2}}\left(\lvert\frac{7}{2},\frac{1}{2}\rangle \mp \lvert\frac{7}{2},-\frac{1}{2}\rangle\right)$; $\frac{1}{\sqrt{2}}\left(\mp\lvert\frac{7}{2},\frac{7}{2}\rangle + \lvert\frac{7}{2},-\frac{7}{2}\rangle\right)$
G_2	$\frac{3}{2}$	$\frac{1}{\sqrt{2}}\left(\lvert\frac{3}{2},\frac{3}{2}\rangle \pm \lvert\frac{3}{2},-\frac{3}{2}\rangle\right)$	$\frac{1}{\sqrt{2}}\left(\lvert\frac{3}{2},\frac{3}{2}\rangle \mp \lvert\frac{3}{2},-\frac{3}{2}\rangle\right)$
	$\frac{5}{2}$	$\frac{1}{\sqrt{2}}\left(\lvert\frac{5}{2},\frac{3}{2}\rangle \mp \lvert\frac{5}{2},-\frac{3}{2}\rangle\right)$; $\frac{1}{\sqrt{2}}\left(\mp\lvert\frac{5}{2},\frac{5}{2}\rangle + \lvert\frac{5}{2},-\frac{5}{2}\rangle\right)$	$\frac{1}{\sqrt{2}}\left(\lvert\frac{5}{2},\frac{3}{2}\rangle \pm \lvert\frac{5}{2},-\frac{3}{2}\rangle\right)$; $\frac{1}{\sqrt{2}}\left(\pm\lvert\frac{5}{2},\frac{5}{2}\rangle + \lvert\frac{5}{2},-\frac{5}{2}\rangle\right)$
	$\frac{7}{2}$	$\frac{1}{\sqrt{2}}\left(\lvert\frac{7}{2},\frac{3}{2}\rangle \pm \lvert\frac{7}{2},-\frac{3}{2}\rangle\right)$; $\frac{1}{\sqrt{2}}\left(\pm\lvert\frac{7}{2},\frac{5}{2}\rangle + \lvert\frac{7}{2},-\frac{5}{2}\rangle\right)$	$\frac{1}{\sqrt{2}}\left(\lvert\frac{7}{2},\frac{3}{2}\rangle \mp \lvert\frac{7}{2},-\frac{3}{2}\rangle\right)$; $\frac{1}{\sqrt{2}}\left(\mp\lvert\frac{7}{2},\frac{5}{2}\rangle + \lvert\frac{7}{2},-\frac{5}{2}\rangle\right)$

TABLE XVI. Basis vectors for the ${}^2C_{4v}$ group for total angular momentum up to $J = 4$. The two-dimensional irreps (E, G_1, G_2) have two components indicated by upper/lower signs. Some irreps have two vectors for certain J values (multiplicities) indicated by semicolomns.

using Table XIII. Note that this table only displays elements that are proper rotations for both O and ${}^2O$. The full symmetry groups O_h and ${}^2O_h$ include the inversion (sometimes called improper rotations). For C_{4v}, the 8 operations are $1(I), 3(iC_{2x} = \sigma_{v1}), 4(iC_{2y} = \sigma_{v2}), 5(C_{2z}), 27(C_{4z}^{+}), 30(C_{4z}^{-}), 37(iC_{2a}^{+} = \sigma_{d1}), 38(iC_{2b}^{+} = \sigma_{d2})$ where we have used the label i to indicate the inversion and give its equivalent names. For the double group ${}^2C_{4v}$, the 16 equivalent operations are $1, 2, 3, 4, 5, 6, 7, 8, 27, 30, 33, 36, 37, 38, 43, 44$. If we call these operations S_k, they all satisfy $S_k\boldsymbol{d} = \boldsymbol{d}$; that is, they preserve the boost direction, which is a general requirement for scattering between unequal-mass particles. For equal masses, the inversion symmetry is restored, so that the boundary conditions are the same for $\pm\boldsymbol{d}$. The little group is enlarged so that the elements obey $S_k\boldsymbol{d} = \pm\boldsymbol{d}$ and the group can be factorized into a direct product of proper transformation and the inversion group.

The C_{4v} group has five irreps conventionally called A_1, A_2, E, B_1, B_2 with respective dimensions $1, 1, 2, 1, 1$. Its double cover group ${}^2C_{4v}$ has seven irreps called $A_1, A_2, E, B_1, B_2, G_1, G_2$ with respective dimensions $1, 1, 2, 1, 1, 2, 2$. It turns out that the ${}^2C_{4v}$ group is isomorphic to the ${}^2D_4$ group (same for the single version C_{4v} to D_4); both belong in the dihedral group family [17]. They have the same irreps and characters, thus the same angular momentum content. The difference is they have different basis vectors. The $^2D_4$ group consists only of proper rotations. The $^2C_{4v}$ group has elements that involve parity transformations. Only proper rotations about the z-axis survive in $^2C_{4v}$, while proper rotations about all three axes (x, y, z) are present in $^2D_4$. The rotations about x and y axis change parity. Consequently, the A_1 irrep of $^2C_{4v}$ group (which is the 'identity' irrep of the group) couples to all possible values of l, but the A_2 irrep only couples to even values starting at $J = 4$. The full basis vectors for the $^2C_{4v}$ group up to $J = 4$ are given in Table XVI. We separate them into two branches, one for even l, one for odd l, but they should be used as one combined basis. The l values are implicit: for integer irreps $l = J$ (assuming two spin-0 mesons); for half-integer irreps $l = J \pm 1/2$. So the basis vectors for G_1 and G_2 in the two branches are distinct, corresponding to two l values (one even, one odd). When the full basis is used in the reduction of phaseshifts, the results in Table VIII and Table IX are obtained.

[1] Martin Lüscher, "Two particle states on a torus and their relation to the scattering matrix," Nucl.Phys. **B354**, 531–578 (1991).

[2] K. Rummukainen and Steven A. Gottlieb, "Resonance scattering phase shifts on a nonrest frame lattice," Nucl. Phys. **B450**, 397–436 (1995), arXiv:hep-lat/9503028 [hep-lat].

[3] Ziwen Fu, "Rummukainen-Gottlieb's formula on two-particle system with different mass," Phys. Rev. **D85**, 014506 (2012), arXiv:1110.0319 [hep-lat].

[4] Luka Leskovec and Sasa Prelovsek, "Scattering phase shifts for two particles of different mass and non-zero total momentum in lattice QCD," Phys. Rev. **D85**, 114507 (2012), arXiv:1202.2145 [hep-lat].

[5] M. Gockeler, R. Horsley, M. Lage, U. G. Meissner, P. E. L. Rakow, A. Rusetsky, G. Schierholz, and J. M. Zanotti, "Scattering phases for meson and baryon resonances on general moving-frame lattices," Phys. Rev. **D86**, 094513 (2012), arXiv:1206.4141 [hep-lat].

[6] Xu Feng, Xin Li, and Chuan Liu, "Two particle states in an asymmetric box and the elastic scattering phases," Phys.Rev. **D70**, 014505 (2004), arXiv:hep-lat/0404001 [hep-lat].

[7] Ning Li and Chuan Liu, "Generalized Lüscher formula in multichannel baryon-meson scattering," Phys. Rev. **D87**, 014502 (2013), arXiv:1209.2201 [hep-lat].

[8] Raul A. Briceno, "Two-particle multichannel systems in a finite volume with arbitrary spin," Phys. Rev. **D89**, 074507 (2014), arXiv:1401.3312 [hep-lat].

[9] Dehua Guo, Andrei Alexandru, Raquel Molina, and Michael Döring, "Rho resonance parameters from lattice QCD," Phys. Rev. **D94**, 034501 (2016), arXiv:1605.03993 [hep-lat].

[10] Craig Pelissier and Andrei Alexandru, "Resonance parameters of the rho-meson from asymmetrical lattices," Phys.Rev. **D87**, 014503 (2013), arXiv:1211.0092 [hep-lat].

[11] R.C. Johnson, "Angular momentum on a lattice," Phys.Lett. **114B** (1982).

[12] David C. Moore and George Tamminga Fleming, "Angular momentum on the lattice: The Case of non-zero linear momentum," Phys.Rev. **D73**, 014504 (2006).

[13] M. Tinkham, *Group theory and quantum mechanics* (Dover, 1964).

[14] Veronique Bernard, Michael Lage, Ulf-G. Meissner, and Akaki Rusetsky, "Resonance properties from the finite-volume energy spectrum," JHEP **08**, 024 (2008), arXiv:0806.4495 [hep-lat].

[15] S.L. Altmann and P. Herzig, *Point-group theory tables* (Oxford University Press, 1994).

[16] S.L. Altmann, *Rotations, quanterions, and double groups* (Dover, 1986).

[17] J.Q. Chen, J.L. Ping, and F. Wang, *Group representation theory for physicists* (World Scientific, 2002).